CrystEngComm

HIGHLIGHT

View Article Online
View Journal | View Issue

Cite this: *CrystEngComm*, 2024, **26**, 3998

Multiple synthesis routes for atomically precise noble metal nanoclusters

Lizhong He †*[ab] and Tingting Dong†[c]

Well-defined metal nanoclusters protected by thiolates, with sizes between nanocrystals and metal atoms, have attracted enormous attention due to their various structures, controllable compositions, intriguing physical and chemical properties, and potential applications. Atomically precise metal nanoclusters are a type of important nanomaterial that can provide an ideal platform to address some key challenges related to their applications. However, compared to the straightforward synthesis of larger nanoparticles, the preparation of ultra-small metal nanoclusters frequently encounters difficulties owing to the pursuit of monodispersity and atomic accuracy. Although a series of effective synthesis methods have been developed for metal nanoclusters with well-defined sizes, structures and compositions, rational design and successful preparation of atomically precise metal nanoclusters still face challenges that further hinder the enrichment of cluster libraries and the in-depth understanding of structure–property relationships. In this review, we summarize some recent advances in strategies for the synthesis of atomically precise metal nanoclusters, in particular, silver and gold nanoclusters as well as alloy nanoclusters, and emphasize the following synthesis methods including the Brust–Schiffrin method, ligand-exchange, galvanic/anti-galvanic reaction, etching, solid phase synthesis and intercluster reaction.

Received 15th May 2024,
Accepted 19th June 2024

DOI: 10.1039/d4ce00488d

rsc.li/crystengcomm

1. Introduction

Generally, ultrasmall metal nanoparticles (less than 3 nm in size, so-called nanoclusters), including gold and silver nanoclusters, consist of several to a few hundred metal atoms with a diameter of about the Fermi wavelength of an electron and represent a new type of aggregation material comprising a metal core and an organic ligand shell.[1–11] Owing to their unique structure and size, nanoparticles show characteristic quantum confinement effects, which lead to their discrete energy levels and molecular-like physicochemical properties, such as strong fluorescence with high QYs, HOMO–LUMO transitions, molecular magnetism, chirality, and so on.[12–27] These attractive properties of sub-nanometer sized metal nanoclusters are distinctively different from those of their larger counterparts, and make these clusters ideal nanomaterials which are widely used in potential applications ranging from biological imaging to optical devices and energy conversion.[28–41]

For metal nanoclusters, the fine control of inherent features, including the size, shape, composition, state of aggregation, atomic packing model and crystallographic arrangement, can effectively tailor their properties.[42–53] Normally, replacing the central metal atom in the inner structure (*e.g.*, core) of a cluster with a heteroatom (*e.g.*, Au, Pt, Pd, Cu, Cr and Pd) can affect the optical (absorption and fluorescence) properties and HOMO–LUMO gaps owing to the synergistic effect on electronic perturbation induced by the incoming atom.[54–66] Meanwhile, tuning the outer structure of clusters, which is enclosed by an outer protecting ligand, is also meaningful for metal nanoclusters for specific applications, albeit all the difficulties.[67–74] Besides, modifying the type of organic ligand and bonding models on the periphery of the clusters is also a crucial step to render their unique properties.[75–84] Only by successfully realizing the controllable synthesis and structural manipulation of atomically precise metal nanoclusters at the atomic level can researchers deeply understand the structure–property correlation of the clusters and ultimately achieve the purpose of cluster practical application.[85–93] At present, the most feasible strategy to control all of these intriguing properties related to the unique structural features of these clusters is to design a suitable synthesis method. Nevertheless, dexterously

[a] *School of Materials Science and Engineering, Xi'an Polytechnic University, Xi'an, 710048, PR China. E-mail: lzhe@xpu.edu.cn*
[b] *Institute of Solid State Physics, Chinese Academy of Sciences, Hefei 230031, PR China*
[c] *School of Environmental Science and Engineering, Shaanxi University of Science and Technology, Xi'an, 710021, Shaanxi, PR China*
† L. H. and T. D. contributed equally to this work.

designing and synthesizing metal nanoclusters remain a major challenge owing to the lack of synthesis approaches.

The synthetic chemistry of atomically precise metal nanoclusters has been explored for a long time, and a large number of excellent studies in the field of cluster synthesis have been reported.[1,2,94–100] Therefore, it is important to highlight the research progress on the controllable synthesis of metal nanoclusters. This review aims to conduct a comprehensive summary of the recent synthesis advances in atomically precise metal nanoclusters, in particular silver, gold and alloy clusters, based on the Brust–Schiffrin method, ligand-exchange, galvanic/anti-galvanic reaction, etching, solid phase synthesis and intercluster reaction (Scheme 1).

2. Brust–Schiffrin method

The first described method, the Brust–Schiffrin method, is a simple and conventional method used for generation of highly purified nanoclusters with a high production rate. The pioneering work could be traced back to 1994 when a great breakthrough in the synthesis of gold nanoclusters was achieved by Brust and Schirrin.[101] Since then, the popular synthesis method has been widely used to prepare air stable, readily soluble, and isolable metal nanoclusters. After decades of development, the original Brust–Schiffrin method gradually evolved into two variants, including a two-phase system in pure water and a toluene solvent and a modified one-phase system (Fig. 1).[102–112] Generally, gold nanoclusters, such as the "star cluster"-Au_{25},[113–125] can be prepared *via* the two-phase method, but silver nanoclusters are formed using the modified one-phase method.[126–135] In detail, the two-phase Brust–Schiffrin method consists of two steps. In the first step, the gold ion provided by the gold salt is sufficiently dissolved in an aqueous solution and the resulting solution further acts as the metal precursor, and then the precursor is transferred to an organic phase under the action of the presence of phase-transfer agents, such as typically tetraoctylammonium bromide. In the second step, both the capping agent (thiolate) and reducing agent (*e.g.* sodium borohydride) are added in succession to the organic solution to prepare the charge-neutral target nanoclusters capped with thiols. In other words, two steps are employed in the two-phase Brust–Schiffrin method, which are transfer of the metal precursor (eqn (1)) and reduction of the target metal ions (eqn (2)).[101,102,109–111]

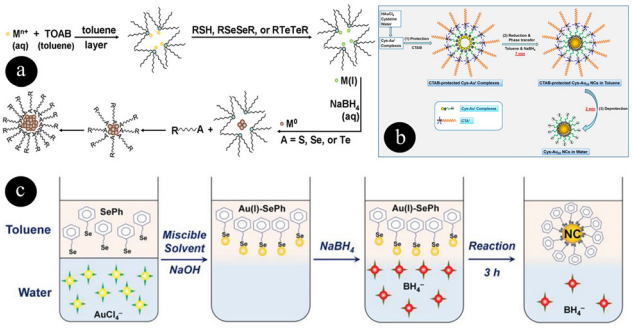

Fig. 1 (a) Schematic illustration of the synthesis of chalcogenate-protected gold nanoclusters by the Brust–Schiffrin method. Reproduced with permission from ref. 103. Copyright 2011, American Chemical Society. (b) Illustrative diagram of the synthesis of hydrophilic CTAB capped Au_{25} nanoclusters *via* two-phase protection deprotection. Reproduced with permission from ref. 104. Copyright 2012, American Chemical Society. (c) The route for preparation of selenolated gold nanoclusters by the solvent-directed phase transfer method. Reproduced with permission from ref. 110. Copyright 2020, Wiley-VCH.

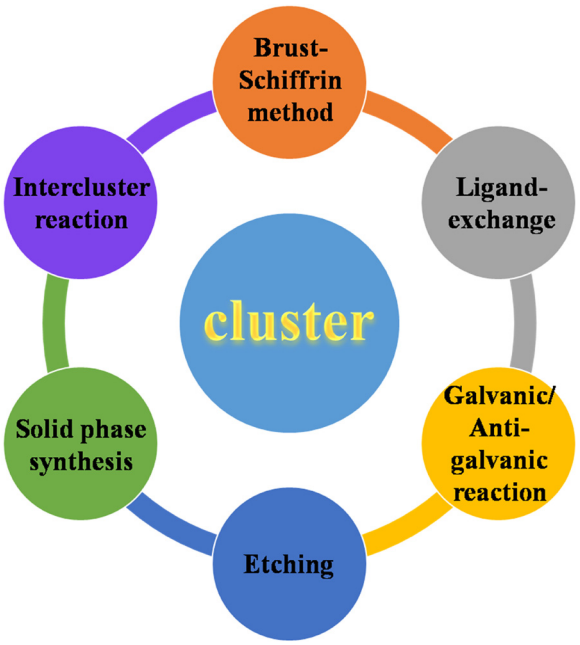

Scheme 1 Schematic representation of multiple routes for controlled synthesis of monodisperse metal nanoclusters.

$$AuCl_4^-\ (aq) + N(C_8H_{17})_4^+\ (toluene) \rightarrow N(C_8H_{17})_4^+AuCl_4^-\ (toluene) \quad (1)$$

$$mAuCl_4^-\ (toluene) + nC_{12}H_{25}SH\ (toluene) + 3me^- \rightarrow 4m\ Cl^-\ (aq) + (Au_m)(C_{12}H_{25}SH)_n\ (toluene) \quad (2)$$

The synthesis mechanism of the two-phase method was studied for a long time because having an insight into the mechanism helps us understand the nucleation mechanisms, growth patterns and passivation procedures in this process of synthesis and even design novel routes for synthesizing other nanoclusters with a high yield. As for the detailed mechanism of the two-phase method, the majority view was that the addition of the capping agent reduces the Au^{3+} to Au^+ and forms $[Au(I)\text{-}SR]_n$-like intermediate polymers, but some excellent studies held different opinions. For example, the types of precursors in the process of the two-phase system were specifically identified and quantified for metal systems (such as Au, Ag, and Cu) by Goulet and co-workers.[136] They found that tetraalkylammonium metal complexes were proved to be the precursors of the two-phase reactions, which differed from

the widely accepted assumptions, but for the one-phase reactions, M(I) thiolates were shown to be the precursors based on the NMR results. Tong *et al.* successfully studied the reaction solution compositions in the well-known two-phase synthesis process after addition of the capping ligand and strong reducing agent *via* multiple techniques, including Raman, NMR, and surface plasmon resonance (SPR) analysis techniques.[103] Finally, they made a conclusion that there was no metal–sulfur bond formation in the organic reaction solution before addition of the reducing agent, and the two-phase system was actually a reverse micellar synthesis method, which was also beneficial to the synthesis of other metals, including Ag and Cu.

Another highlight of the Brust–Schiffrin method is to prepare alloy nanoclusters. And this method has gradually developed into a mainstream method for preparing alloy nanoclusters. As early as 2009, Murray's group prepared small monolayer-capped AuPd nanoclusters using this method, which were determined to be $Au_{24}Pd(SC_2Ph)_{18}$ based on positive mode electrospray ionization mass spectrometry (ESI-MS).[137] Also, Negishi *et al.* synthesized $Au_{25-x}Ag_x(SC_{12}H_{25})_{18}$ bimetal nanoclusters with different Ag–Ag mixing ratios in a binary reaction system.[138] Initially, after mixing the aqueous solution of gold and silver salts with various molar ratios (22 : 3, 19 : 6, 15 : 10, 10 : 15, 8 : 17 and 5 : 20, respectively), a toluene solution of the phase transfer agent was introduced into the reaction system. When the two phases were separated, a capping agent was added into the separated toluene solution. By reducing the metal–thiolate complexes, nanoclusters were obtained. By the way, the physical properties and electronic structure of $Au_{25-x}Ag_x(SC_{12}H_{25})_{18}$ could be continuously tailored by the doped Ag atoms. Similarly, based on this proposed protocol, Xie's group also synthesized a series of fluorescent alloy nanoclusters capped with hydrophilic ligands.[139]

Besides, Brust *et al.* also extended this well-known method to the synthesis of gold nanoclusters using *p*-mercaptophenol as a capping agent in a one phase system, which paved the way for the synthesis of various metal nanoclusters (Au, Ag, Cu, Pt) protected by a variety of ligands.[140] Compared to the two-phase method, the one phase method is simple and versatile. For example, Wu and co-workers designed a one-phase method for synthesizing monodisperse thiolate-protected Ag_7 clusters using *meso*-2,3-dimercaptosuccinic acid (DMSA) as the surface stabilizer.[106] In the typical synthesis, silver nitrate used as the silver source was dissolved in an ethanol solution and was cooled to 0° in an ice bath. $Ag_x(DMSA)_y$ intermediate complexes were formed after addition of DMSA under medium–low speed stirring, and then the intermediates were reduced by solid powder $NaBH_4$ under intense stirring. Finally, monodisperse Ag_7 nanoclusters were obtained after 12 h of reaction. In their another study, they prepared a highly pure atomically monodisperse Au_{25} nanoclusters capped with different functionalized surface ligands using a modified one-pot method together with a "size-focusing" process.[141] The THF-mediated one-pot synthetic method in this report at least has two obvious merits compared to the conventional two-phase synthetic protocols and ligand-exchange method. On the one hand, the modified one-pot method significantly improves the purity of the Au_{25} nanocluster product compared to the approach using ethanol as a solvent. On the other hand, this synthetic strategy provides a more simple and convenient access to generation of functionalized Au_{25} and even other metal nanoclusters using hydrophilic or hydrophobic surface functionalities. Using a similar approach, Negishi *et al.* prepared small sized monolayer-protected gold nanoclusters *via* the reducibility and stability of the capping agent (DMSA).[142] The results from the compositional analysis showed that DMSA-stabilized monodisperse gold nanoclusters consist of 10–13 atoms. After the success in synthesizing the star nanoclusters, such as Au_{25} (ref. 34, 107 and 113–125) and Au_{38} (ref. 102, 109 and 143–149) nanoclusters, a series of atomically precise $Au_n(SR)_m$ (ref. 88, 89 and 150–157) and $Ag_n(SR)_m$ (ref. 61, 65 and 158–165) and other metal nanoclusters[47,166–170] were obtained in high yield and on a large scale, using the above-mentioned synthetic routes.

3. Ligand-exchange

Besides the initial and modified Brust–Schiffrin methods, ligand exchange is another good strategy to tailor the electronic and geometric structure (including core and shell structures) of ligand protected metal nanoclusters.[171–176] Up to now, the ligand exchange method mainly involves two aspects: the ligand exchange reaction from phosphine-protected (thiol-protected) metal nanoclusters to new (thiol-protected) phosphine-protected metal nanoclusters[177,178] and the ligand exchange reaction from thiol-protected metal nanoclusters to new thiol-protected metal nanoclusters.[172,179–186] The driving forces of ligand exchange, however, are completely different for these two types of ligand capped metal nanoclusters.[175] For the former, the difference in bonding abilities and coordination modes between the metal–P and metal–S are the decisive driving force of the ligand-exchange reactions. For the latter, the internal dynamics of reactions involves several factors, including the inherent properties (steric hindrance, rigidity, *etc.*) between the different thiol ligands and modulating factors (*e.g.*, reaction temperature), as well as the fundamental characteristics (size, composition, structure, *etc.*) of the nanoclusters. According to the literature, PPh_3-stabilized and narrow-sized gold nanoclusters were one of the earliest studied nanomaterials using this approach.[177] As early as 1997, Hutchison and co-workers demonstrated that $Au_{55}(PPh_3)_{12}Cl_6$ nanoclusters could be transformed into thiol-stabilized 1.7 nm diameter gold clusters with controlled ligand exchange.[187] The ligand exchange reaction was achieved by stirring the parent Au_{55} nanoclusters in the presence of excess thiol that included 1-propanethiol, 1-octadecanethiol, and 4-mercaptobiphenyl in dry dichloromethane, and the produced gold nanoclusters had excellent thermal and air stability. For a ligand-exchange

approach, the critical factors in the process of reactions are the accurate control of thiol dosage and the reaction time, because high thiol/atom molar ratios and a prolonged reaction may cause the decomposition of the target nanoclusters, and low thiol to atom ratios and a short time reaction may lead to incomplete reactions. Although the major reaction factors (*e.g.*, temperature, reaction time and added thiol dose) of the ligand exchange procedure need to be strictly regulated, this method is widely used in the following aspects:

(i) Induced structural transformation of nanoclusters. For example, using the atomically precise pure $Au_{38}(PET)_{24}$ as the starting nanoclusters, Zeng *et al.* synthesized new stable $Au_{36}(TBBT)_{24}$ nanoclusters through the thiol-to-thiol ligand exchange. Interestingly, the crystal structure of the produced $Au_{36}(TBBT)_{24}$ was completely different from that of the parent nanoclusters (Fig. 2(a)).[180,188] The parent Au_{38} nanoclusters contained a rod-like face-sharing biicosahedral Au_{23} core capped by three (–SR–Au–SR–) monomer staple motifs and six (–SR–Au–SR–Au–SR–) dimer staple motifs whereas the produced Au_{36} nanocluster adopted a more peculiar structure with a truncated tetrahedral face-centered-cubic (fcc) Au_{28} core and four traditional dimer staple motifs and 12 bridging thiolates. Because this is a groundbreaking study that has a positive effect on the more synthetic fields in nanochemistry, we outline below the basic steps or features and mechanism of this method. Based on the analysis of the MS and UV-vis curves as well as the crystal structures, the transformation mechanism of Au_{38} to Au_{36} was proposed. The total ligand exchange reaction could be divided into four stages: (i) the ligand exchange reaction was triggered by the new added TBBT thiol, and up to 12 TBBT ligands were successfully exchanged onto the surface of Au_{38} during the first 5 minutes. (ii) The ligand exchange reaction continued and the population of exchange product $Au_{38}(TBBT)_m(PET)_{24-m}$ increased. (iii) This stage was very important because of the transformation of $Au^*_{38}(SR)_{24}$ (Au^*_{38} denoting the distorted structure) to $Au_{36}(SR)_{24}$ and $Au_{40}(SR)_{26}$ and a disproportionation reaction process was identified. (iv) A size conversion occurred together with further ligand exchange toward completion and all of the intermediate clusters which included Au_{40} and Au_{38} were converted to the stable $Au_{36}(SR)_{24}$ nanoclusters. Additionally, the transformation between the structural isomers ($(Au_{28}(S\text{-}c\text{-}C_6H_{11})_{20}$ *vs.* $Au_{28}(SPh^t\text{-}Bu)_{20}$) has been achieved through the ligand exchange approach.[189] In a typical synthetic process, the $Au_{28}(SPh^tBu)_{20}$ nanoclusters were reacted with excess cyclohexanethiol for 2 h at 80 °C, and then novel Au_{28} nanoclusters with quasi-D_2 symmetry were obtained. Interestingly, the reversible transformation can be also achieved between the two gold nanoclusters with isomeric structures *via* ligand exchange at a high reaction temperature. The theoretical analysis showed that the ligand effects were responsible for the ligand-induced isomerization process and thermal stability of the two gold nanoclusters. In addition to the structural transformation between the two gold nanoclusters, structural inter-conversion among three fcc- and non-fcc-structured gold nanoclusters, including $Au_{44}(SPh^tBu)_{28}$, $Au_{44}(SPhMe_2)_{26}$, and $Au_{43}(S\text{-}c\text{-}C_6H_{11})_{25}$ nanoclusters, has also been achieved by Wu's group using the ligand exchange.[48] From a structural point of view, such structural transformation from an fcc structure to a non-fcc structure was accomplished for the first time. Apart from the gold nanoclusters, the structural transformation in the silver nanocluster field has also made remarkable achievements. For example, Bakr and co-workers investigated the reversible inter-conversion between hollow $Ag_{44}(SPhF)_{30}$ and nonhollow $Ag_{25}(SPhMe_2)_{18}$ nanoclusters (Fig. 2(d)).[173] Taking the transformation of Ag_{44} to Ag_{25} as an example to illustrate the mechanism during the reaction progress, this total conversion procedure was summarized into four parts: (step 1) up to 18 SPhF on the surface of the parent $Ag_{44}(SPhF)_{30}$

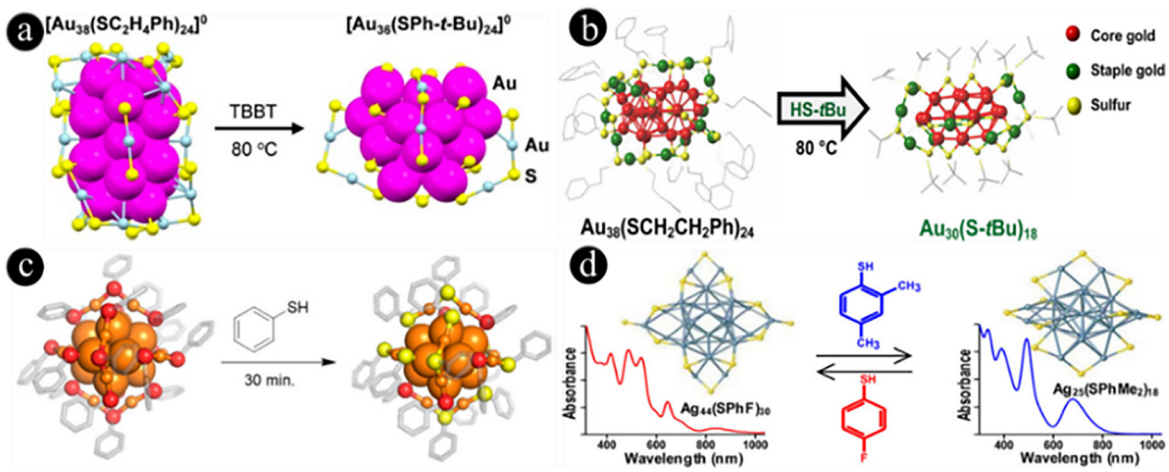

Fig. 2 (a) Nanocluster transformation from Au_{38} to Au_{36}. Reproduced with permission from ref. 180. Copyright 2013, American Chemical Society. (b) Nanocluster transformation from Au_{38} to Au_{30}. Reproduced with permission from ref. 197. Copyright 2017, American Chemical Society. (c) Selective partial substitution of thiolate on the surface of Au_{25} nanoclusters by the selenolate ligand. Reproduced with permission from ref. 186. Copyright 2019, American Chemical Society. (d) Reversible transformation of the structure between Ag_{44} and Ag_{25}. Reproduced with permission from ref. 173. Copyright 2016, American Chemical Society.

nanoclusters were replaced by the new $SPhMe_2$ ligands and the main product $Ag_{44}(SPhF)_{12}(SPhMe_2)_{18}$ was produced. (Step 2) $Ag_{44}(SPhF)_1(SPhMe_2)_{29}$ became the most predominant product. (Step 3) the distorted $Ag_{44}(SPhF)_1(SPhMe_2)_{29}$ was dissociated disproportionately to form mixed ligand protected $Ag_{25}(SPhF)_1(SPhMe_2)_{17}$. And (step 4) all of the intermediates, including Ag_{46}, Ag_{48} and Ag_{50}, were decomposed to $Ag_{25}(SPhF)_1(SPhMe_2)_{17}$, and finally $Ag_{25}(SPhMe_2)_{18}$ was obtained. Besides, structural transformation has also been achieved from thiol protected silver nanoclusters to Se-donor ligand protected silver nanoclusters. Liu's group exchanged $Ag_{20}\{S_2P(O^iPr)_2\}_{12}$ and $Ag_{21}\{S_2P(O^iPr)_2\}_{12}$ with Se-donor ligands,[190] giving rise to $Ag_{20}\{Se_2P(O^iPr)_2\}_{12}$ and $Ag_{21}\{Se_2P(OEt)_2\}_{12}$, respectively. A THF suspension of $Ag_{20}\{S_2P(O^iPr)_2\}_{12}$ was reacted with an excess of $NH_4[Se_2P(O^iPr)_2]$ for less than 1 minute and then the target nanoclusters were separated from the mixtures. Structurally, $Ag_{20}\{Se_2P(O^iPr)_2\}_{12}$ consisted of a centered icosahedral Ag_{13} kernel and 7 capping Ag atoms and 12 dsep ligands. However, cluster $Ag_{21}\{Se_2P(OEt)_2\}_{12}$ with four three-fold rotational axes contained an Ag_{21} core and 12 ligands and the packing of these clusters displayed the same bridging pattern of trimetallic tri-connectivity with one core Ag atom and two ligand Ag atoms. In general, using the ligand exchange, the structural change between the gold/silver nanoclusters can be implemented under the optimal conditions. Numerous excellent cases have been reported (Fig. 2), including the size (structure) transformation of $Au_{329}(SC_2H_4Ph)_{84}$ to $Au_{279}(SPh^tBu)_{84}$,[183] $Au_{144}(SC_2H_4Ph)_{60}$ to $Au_{99}(SPh)_{42}$,[191] $Au_{144}(SC_2H_4Ph)_{60}$ to $Au_{133}(SPh^tBu)_{52}$,[192] $Au_{25}(SC_2H_4Ph)_{18}$ to $Au_{20}(SPh^tBu)_{16}$,[193] $Au_{25}(PET)_{18}$ to $Au_{28}(TBBT)_{20}$,[194] $Au_{25}(SC_2H_4Ph)_{18}$ to $Au_{24}(SC_2H_4Ph)_{20}$,[195] $Au_{23}(S\text{-}c\text{-}C_6H_{11})_{16}$ to $Au_{24}(SCH_2Ph^tBu)_{20}$,[196] $Au_{38}(SC_2H_4Ph)_{24}$ to $Au_{30}(S^tBu)_{18}$,[197] $Au_{60}S_6(SCH_2Ph)_{36}$ to $Au_{60}S_7(SCH_2Ph)_{36}$,[198] $Au_{30}(S^tBu)_{18}$ to $Au_{36}(SPhX)_{24}$,[199] $Ag_{44}(p\text{-}MBA)_{30}$ to $Ag_{50}(dppm)_6(SCH_2Ph^tBu)_{30}$,[49] $Ag_{51}(SSR)_{19}(PPh_3)_3$ to $Ag_{29}(SSR)_{12}(PPh_3)_4$,[200] $Ag_{59}(SPhCl_2)_{32}$ to $Ag_{44}(SPhF)_{30}$,[201] $Ag_{59}(SPhCl_2)_{32}$ to $Ag_{25}(SPhMe_2)_{18}$,[201] and $Ag_{44}(SPhF)_{30}$ to $Ag_{37}(SG)_{21}$.[202]

(ii) Induced phase transfer of nanoclusters. Ligand exchange has also been utilized as an important strategy for the phase transfer. For example, by ligand exchanging phosphine-stabilized Au_{11} nanoclusters with a water-soluble thiol (GSH), Tsukuda and coworkers synthesized $Au_{25}(SG)_{18}$ nanoclusters with well-defined compositions on a large scale under the optimized conditions.[103] One reason why GSH protected metal nanoclusters could react with the free thiol might be that the hydrophobic ligand could accelerate the decomposition of the GSH ligand capped multiple-disperse nanoclusters in the two-phase system under the optimal conditions (*e.g.* at an elevated temperature or pressure), and various intermediate clusters were formed during the ligand exchange process, and finally the most stable metal nanoclusters survived after a spontaneous "size-focusing" procedure. Qian *et al.* reported a facile and large-scale synthesis of hydrophobic ligand stabilized monodisperse Au_{38} nanoclusters in high purity through the ligand exchange reaction of glutathione-protected Au_n nanoclusters with the dodecanethiol ligand.[203] After the reactions finished, no GSH ligands were located on the surface of the obtained Au_{38} clusters, suggesting that the transformation between the two clusters was complete. Using the same method, Jin *et al.* also prepared monodisperse hydrophobic $Ag_{62}S_{12}(SBu^t)_{32}$ nanoclusters through exchanging the hydrophilic $Ag_n(SG)_m$ clusters with the tert-butyl mercaptan capping agent in a biphase system at ambient temperature.[204]

(iii) Induced functionalization of nanoclusters. The ligand exchange approach is also an efficient method to prepare multifunctional metal nanoclusters (fluorescence and catalysis). An excellent case in nanocluster functionalization was provided by Pradeep's group.[205] In 2008, Shibu from this group exchanged the ligand of glutathione thiolate protected Au_{25} with two kinds of ligands which included 3-mercapto-2-butanol (MB) and *N*-acetyl- and *N*-formyl-glutathione (NAGSH and NFGSH, respectively) to tune the optical and photoluminescence properties of the clusters. Compared to the parent $Au_{25}(SG)_{18}$ nanoclusters, the optical absorption properties of all the nanoclusters were similar and there was no change in the chemical nature of the metal core. Although the inherent fluorescence and solid-state emission of these clusters were observed, the excitation spectra of the MB-exchanged clusters and the acetyl- and formyl-glutathione exchanged products were remarkably different. Additionally, Zhao and coworkers prepared novel adamantanethiolate-protected $Au_{40}(S\text{-}Adm)_{22}$ nanoclusters and introduced a water-soluble component, γ-CD-MOF, into the hydrophobic ligand to endow the thiol protected gold nanoclusters with excellent aqueous phase catalytic activity in a horseradish peroxidase-mimicking reaction system.[206]

In 2017, Zhu's group proposed an *in situ* two-phase exchange method, which combined the merits of the simple one-pot approach and the efficient two-phase ligand-exchange method.[207] This developed method is also very suitable for the preparation of alloy nanoclusters with well-defined structures. In detail, various ingredients, including metal salts ($AgNO_3$ and $HauCl_4$) and the water-soluble GSH ligand, were mixed and stirred in a heated aqueous solution, forming GSH-capped bimetal alloy nanoclusters in a short amount of time. Subsequently, a toluene solution containing a dose of *tert*-butylamine complex and *tert*-butyl mercaptan was added into the above water phase reaction system, which could facilitate the *in situ* two-phase exchange from the GSH-capped AgAu alloy nanoclusters to a series of thiolate-capped alloy nanoclusters, such as $Au_{20}Ag_1(SR)_{15}$ (NC-1), $Au_{21-x}Ag_x(SR)_{15}$ (x = 4–8), $Au_{21-x}Cu_x(SR)_{15}$ (x = 0 or 1), and $Au_{21-x}Cu_x(SR)_{15}$ (x = 2–5). Although the structure information of the GSH-protected AgAu alloy nanoclusters was unavailable, the frameworks of the thiolated alloy nanoclusters have been determined. More importantly, the authors pointed out that neither the typical one-pot nor the conventional ligand-exchange method could be used to synthesize the target alloy nanoclusters obtained by

this newly proposed method, implying that the *in situ* two-phase exchange method could be used as a powerful alternative for preparing precise alloy nanoclusters. Another representative alloy nanocluster ($Au_{24}Cu_6(SPh^tBu)_{22}$) was also synthesized by Zhu's group using this method.[208]

4. Galvanic/anti-galvanic reaction

The galvanic reaction is a redox process, in which a noble metal ion can be spontaneously reduced by a less noble metal in solution owing to the difference in electrochemical potential.[209] According to the classical metal activity sequence (Zn > Fe > Cd > Co > Ni > Pb > Cu > Ru > Hg > Ag > Pd > Ir > Pt > Au), the most common example of a galvanic reaction in clusters is that Ag(0) clusters can be oxidized by the Au(III) ion in the gold salt ($HAuCl_4$) through the 3Ag(0) + Au(III) → Au(0) + 3Ag(I) redox reaction process based on the fact that the redox potential of Au(III)/Au(0) is approximately 1 V, which is obviously higher than that of Ag(I)/Ag(0) (Fig. 3(a)).[210,211] Thus, the difference in electrochemical potential acts as the driving force. This method is widely used to prepare alloy nanoclusters by introducing a noble metal ion into a less noble metal cluster. For example, Bootharaju *et al.* demonstrated the atomically precise doping of atom-accurate silver nanoclusters by gold atoms *via* the novel galvanic reaction strategy.[59] In the galvanic reaction process, reacting the pure Ag_{25} cluster with an Au salt precursor ($AuClPPh_3$) gave birth to the formation of the monogold-doped Ag_{25} cluster, and the entire galvanic reaction involving the formation of $AuAg_{24}(SR)_{18}$ (SR = 2,4-dimethylbenzenethiol; 2,4-DMB for short) is shown as follows: $Ag_{25}(SR)_{18}^- + Au^+ \rightarrow AuAg_{24}(SR)_{18}^- + Ag^-$. Compared to the structure of the famous Ag_{25} cluster, the alloy cluster retained the total structure except for the inner core. Based on the results of ESI-MS and X-ray single crystallography, the inserted gold atom was located in the center of the icosahedral Ag_{12} to form the Au@Ag_{13} core, forming the multiple core–shell structure of the Au-doped Ag_{25} cluster. Interestingly, by directly reducing the gold and silver precursors with a reductant in the mixed solvent of DCM and methanol containing the capping agent, a mixture of compositions $Ag_{25-x}Au_x(2,4\text{-DMB})_{18}^-$ (x = 1–8) with the same nominal structural framework was produced. Although the Au^+ feed was varied during the synthetic process, a pure product with monodispersity was not obtained, suggesting the importance of selecting a suitable synthesis approach in preparing the target clusters. The influence of heteroatom doping on the parent cluster was manifested in two aspects: surface structure and properties. On the surface of the mono-doped Ag_{25} cluster, only eight out of eighteen ligands were found to participate in parallel-displaced π–π interactions (distance between both phenyl rings, 3.706–3.725 Å), which was obviously different from the twelve ligands in the pure Ag_{25} cluster. Aside from the structural difference, the photoluminescence of the gold-doped silver nanocluster was improved by a factor of 25 times compared to the pure Ag_{25} cluster, and the ambient stability of the former was also better than the latter, suggesting that the heteroatom doping of monodisperse Ag_{25} could alter the electronic structure and increase the stability of the target cluster. Under the guidance of the galvanic reaction, by introducing the heteroatom (gold atom) into the parent silver cluster, a bimetallic thirteen-atom alloy quantum cluster Ag_7Au_6, which was capped by the mercaptosuccinic acid (H_2MSA) ligand, was obtained by Pradeep and coworkers in 2012.[212] The monodispersity of the cluster was proved by PAGE and its properties were further characterized by multiple techniques including UV/Vis, FTIR, luminescence, TEM, XPS, SEM/EDAX, and ESI MS. Theoretically, one of the possible crystal structures was proposed, and it had a spherical structure in which a distorted icosahedral core with C_{2v} symmetry was capped by a bridged staple of –Au/Ag–SR–Au/Ag–. According to the synthetic procedure, the most crucial step in the synthesis process was that addition of an appropriate amount of gold salt to the parent $Ag_{7,8}$ cluster in the last step produced the final alloy Ag_7Au_6 cluster. Recently, starting from phosphine and thiolate ligand co-protected pure $Ag_{50}(SR)_{30}(DPPM)_6$ (SR = 4-*tert*-butylbenzyl mercaptan), Zhu's group successfully synthesized a medium-sized AgAu alloy cluster ($Ag_{50-n}Au_n(SR)_{30}(DPPM)_6$) *via* the galvanic metal exchange reaction.[49] The X-ray crystallography results showed that both clusters shared a similar structure, and the only difference was that the hollow Ag_{12} core was partially replaced by the gold atoms. Besides, further investigation showed that exchanging the silver atoms by the gold atoms in the core could affect the HOMO–LUMO orbitals and optical absorption properties, as well as stability. In another excellent case, Xie's group reported the surface silver atom exchange between the well-known $Ag_{44}(p\text{-MBA})_{30}^{4-}$ cluster and the preformed Au-pMBA precursor to produce the isomeric $Au_{12}Ag_{32}(p\text{-MBA})_{30}^{4-}$ cluster.[213] Using mass spectrometry to

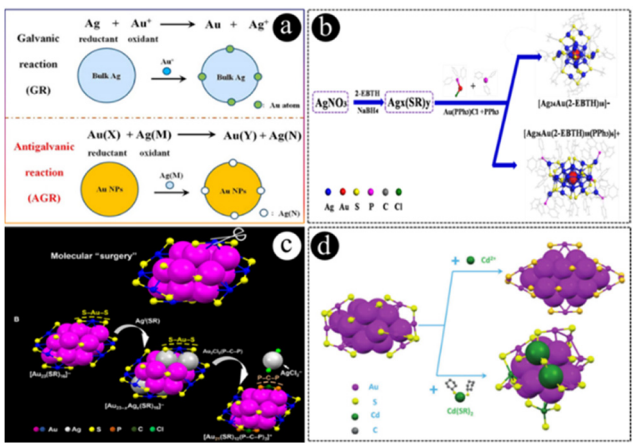

Fig. 3 (a) Schematic illustration of the GR and AGR processes. Reproduced with permission from ref. 210. Copyright 2018, American Chemical Society. (b) Route for preparation of DNIC ($Ag_{26}Au@Ag_{24}Au$). Reproduced with permission from ref. 214. Copyright 2019, John Wiley and Sons. (c) "Molecular surgery" on the Au_{23} cluster *via* the AGR. Reproduced with permission from ref. 51. Copyright 2017, American Chemical Society. (d) Cd^{2+} induced transformation of Au_{23} to Au_{28} *vs.* $Cd(SR)_2$ induced transformation of Au_{23} to $Au_{20}Cd_4$. Reproduced with permission from ref. 219. Copyright 2018, John Wiley and Sons.

track the surface motif exchange (SME) reaction, the results showed that the original surface structure of –SR–Ag–SR– protecting modules of the parent cluster was replaced by the incoming –SR–Au–SR– motifs, leading to the formation of a core–shell alloy nanocluster. Theoretically, the construction of the thermodynamically less favorable core–shell Ag@Au nanocluster could be attributed to the intermediate Ag_{20} shell, which provided a diffusion barrier to prevent surface gold atom inward diffusion. Similarly, an alternating array stacking structure of $Ag_{24}Au$ and $Ag_{26}Au$ clusters, named as a double nanocluster ionic compound (DNIC), was successfully assembled by adding an $Au(PPh_3)Cl$ complex and an auxiliary ligand (PPh_3) into DCM containing multi-sized $Ag_x(SR)_y$ (SR = 2-ethylbenzenethiol) *via* the galvanic metal exchange method (Fig. 3(b)).[214] In the unique crystal structure, the cationic $Ag_{26}Au(SR)_{18}(PPh_3)_6^+$ and anionic $Ag_{24}Au(SR)_{18}^-$ gathered and assembled along the [001] direction using electrostatic interactions with weak interactions (*e.g.*, π–π and C–H–π interactions). The overall geometric structure of $Ag_{26}Au$ was similar to that of the analogue $Ag_{26}Pt(SR)_{18}(PPh_3)_6$ (SR = 2-ethylbenzenethiol) cluster,[45] in which a bipyramid $AuAg_{14}$ core was surrounded by two identical ring-like $Ag_6(SR)_9(PPh_3)_3$ staple motifs, and the framework of $Ag_{24}Au(SR)_{18}$ was identical to that of $Ag_{24}Au(SR)_{18}$ in the single nanocluster ion compound (SNIC).[59,66,215,216] Besides, owing to the multiple non-covalent interactions in the crystal, the fluorescence intensity of the crystalline state of DNIC was higher than that of the amorphous state. Reacting Au–SR complexes with spherical $Ag_{24}Pt(SR)_{18}$ (SR = 2,4-dimethylbenzenethiol) with a precise molecular structure generated the shape-maintained $Au_xAg_{24-x}Pt(SR)_{18}$ ternary alloy cluster.[217] In contrast, by replacing the Au–SR complexes with an $Au(PPh_3)Br$ precursor, the formed ternary alloy cluster was determined to be the rod-like $Au_{10}Ag_{13}Pt_2(PPh_3)_{10}Br_7$ cluster.[218] Based on the structural features of the two ternary alloy nanoclusters, as well as the parent bimetal nanocluster, the authors believed that: (i) the Pt atom in the icosahedron was stable enough to hold the central position; (ii) the phosphine ligand could peel the outer shell of the spherical parent cluster to form the building blocks of rod-like nanoclusters; (iii) the anionic Br^- played a crucial role in assembling the final target nanocluster.

Recently, the anti-galvanic reaction, which is opposite to the classic galvanic reaction, has been regarded as a new and efficient approach to prepare atomically precise alloy nanoclusters.[209] As early as 2010, Murray's group reported that phenylethanethiolate (PET) protected negative Au_{25} clusters could react with silver ions, producing $Au_{24}Ag(PET)_{18}^{2+}$ and $Au_{23}Ag_2(PET)_{18}^{2+}$ alloy nanoclusters, by regulating the ratio of the parent cluster to silver ions, showing that the opposite of the classical galvanic reaction could occur.[220] Later, Wu's group first proposed a general concept of the anti-galvanic reaction (AGR) and confirmed that the AGR is an intrinsic nature of ultrasmall nanoclusters and is associated with several factors including the size of a metal, the type of surface ligand and the ion precursor as well as ion dose, and revealed that, aside from negative Au_{25}, neutral Au_{25} and ultra-small thiolated metal (*e.g.*, silver and gold) nanoparticles with less than 3 nm in size could react with silver or copper ions.[221,222] Since then, the new era of AGRs has begun, which have been considered a new and efficient way for the preparation of alloy nanoclusters.[209,210] For example, Wu's group successfully achieved mono-Hg and mono-Cd atom doping of the well-studied $Au_{25}(PET)_{18}$ cluster by means of the AGR (Fig. 3(d)).[54,123,219,223] One structural feature to be clear for the Cd-doped cluster was that one gold atom on the surface of the icosahedral core of homo-Au_{25} was replaced by the incoming Cd atom, which was obviously different from that of the Hg-doped cluster where one gold atom in the staple motif was replaced by a foreign Hg atom, which was also different from that of the Cd-doped Au_{25} cluster reported by Zhu's group. Interestingly, the $Au_{24}Cd$ cluster could be transformed into the $Au_{24}Hg$ cluster, but the reverse process did not occur owing to the different stability.[224] Zhu's group also prepared thiolated trimetallic $MAg_nAu_{24-n}(PET)_{18}$ (M = Cd or Hg) by replacing the central gold atom with Cd– or Hg–PET complexes. The crystal structure showed that the Cd or Hg atom was located in the central position of the core, and the icosahedral M_{12} consisted of silver–gold bimetallic metals, which was further capped by the staple motifs.[225] Negishi and coworkers synthesized two trimetallic nanoclusters $Au_{\sim20}Ag_{\sim4}Pd(SC_2H_4Ph)_{18}$ and $Au_{\sim20}Ag_{\sim4}Pt(SC_2H_4Ph)_{18}$ by means of the AGR between the neutral $Au_{24}Pd(SC_2H_4Ph)_{18}$ or $Au_{24}Pt(SC_2H_4Ph)_{18}$ and $Ag–SC_2H_4Ph$.[226] The geometries of the trimetallic nanoclusters were similar to those of the spherical M_{25} model such as $Au_{25}(PET)_{18}^{-/0}$, $Au_{24}Pt(PET)_{18}^0$, $Au_{24}Pd(PET)_{18}^0$, $Au_{24-x}Ag_xHg(PET)_{18}^0$, $Au_{25-x}Ag_x(PET)_{18}^-$, and $Au_{24-x}Ag_xCd(PET)_{18}^0$. In both trimetallic clusters, the Pd or Pt atom was situated in the center of the icosahedral core. By combination of an AGR and a quasi-AGR strategy, Jin and coworkers reported a site-specific "surgery" on the surface of atomically precise $Au_{23}(S\text{-}c\text{-}C_6H_{11})_{16}$ to generate a new $Au_{21}(SR)_{12}(P–C–P)_2^+$ (P–C–P = $Ph_2PCH_2PPh_2$) cluster.[51] In the interesting "surgery" reaction, the Au_{23} cluster was sequentially reacted with Ag(I)-SR and $Au_2Cl_2(P–C–P)$ complexes, giving birth to the final target Au_{21} cluster through an intermediate product silver-doped $Au_{23-x}Ag_x(SR)_{16}$ ($x \sim 1$), without changing the structure of the remaining part of the parent cluster. Similarly, Wang *et al.* successfully achieved single metal atom shuttling into and out of the rod-like $Au_{24}(PET)_5(PPh_3)_{10}Cl_2$ cluster by adding the MCl salt (M = Cu/Ag) into DCM containing the parent system.[227] Based on the experimental and theoretical results, they found that the foreign atom could squeeze the pre-existing gold atom of the cluster into the hollow site to transform it into a non-hollow MAu_{24} cluster. In particular, the incoming silver atom was located in the icosahedral vertex of M_{13}, while the copper atom could occupy either the icosahedral vertex (30% population) or waist (70% population) positions of M_{13}. Interestingly, the $AgAu_{23}$ cluster transformed from the centrally hollow Au_{24} could be further converted into the Ag_2Au_{23} cluster in which both silver atoms occupied the apex positions of the cluster and connected with Cl atoms. Besides, a few cases of Cd atom doping of gold nanoclusters were also achieved by means of the AGR, including

$Au_{20}Cd_4(SH)(CHT)_{19}$,[219] $Au_{19}Cd_3(SR)_{18}$ (ref. 228) and $Au_{26}Cd_4(CHT)_{22}$.[223]

5. Etching

Generally, the etching approach can be divided into two categories, physical and chemical etching. Belonging to the regime of "top down" synthetic routes, chemical etching, which consists of ligand etching, acid etching and so on, is more favorable for metal cluster synthesis due to many controllable factors.[229] As early as 2007, using multivalent coordinating polymers to etch preformed high-quality gold nanocrystals (7 nm in size), Nie and coworkers reported an etching process for synthesizing highly fluorescent and water-soluble gold nanoclusters.[230] Although the crystal structure of the target nanocluster was not obtained at that time, the composition was determined to be Au_8 by electrospray ionization (ESI) mass spectrometry. Based on a series of analyses, two possible etching synthesis mechanisms in this process were proposed. One mechanism was that Au_8 clusters were liberated from the nanocrystal surface and immediately protected by a multivalent and hyperbranched PEI ligand; the other was that Au(I) ions were generated during the ligand exchange process and the released Au(I) species were aggregated by the PET ligand. An interesting contribution to preparation of highly fluorescent metal nanoclusters in a mild etching environment was provided by Yuan *et al.* who synthesized stable and monodisperse Au, Ag, Pt and Cu nanoclusters through mild etching of initially unstable, multi-scaled and nonfluorescent parent nanoclusters.[55] The water soluble non-fluorescent parent metal nanoclusters protected by the water soluble glutathione ligand were first prepared using the traditional co-reduction approach under designed conditions, and then the as-obtained parent metal nanoclusters were transferred to a toluene solution in the presence of cetyltrimethylammonium bromide *via* electrostatic interaction between negatively charged carboxyl groups from the GSH ligand on the surface of the metal nanoclusters and positively charged cations of the hydrophobic salt. Finally, the most important step, mild etching, was achieved in the organic phase (toluene solution), giving birth to the formation of highly stable and fluorescent metal nanoclusters. Interestingly, the produced metal nanoclusters could be transferred back to the aqueous phase after removing the cation CAT^+. In addition, Xia *et al.* successfully synthesized novel phenylethanethiolate protected $Au_{38}(PET)_{26}$ nanoclusters by an acid etching synthesis method.[231] In this work, a series of phenylethanethiolate protected nanoparticles in different sizes (including nanoparticles in sizes ~4 nm and ~2 nm, Au_{144}, Au_{38} and Au_{25} nanoclusters) were etched with acetic acid at elevated temperature (80°). Interestingly, Au_{144} nanoclusters and large size Au nanoparticles could not react with the etchant, while smaller sized Au_{38} and Au_{25} could react with the etchant under the same conditions, indicating a size-dependent reactivity of gold nanoparticles with the etchant. Jin *et al.* also reported the synthesis of monodisperse $Au_{144}(SCH_2CH_2Ph)_{60}$ nanoclusters *via* one-phase thiol etching of Au nanocrystals protected by $-SCH_2CH_2Ph$ thiolates (Fig. 4).[232] Although the detailed chemical etching mechanism of the foreign ligand induced medium or larger metal nanoparticle etching has not yet been particularly clear, this method has great potential for the synthesis of small size metal nanoclusters.

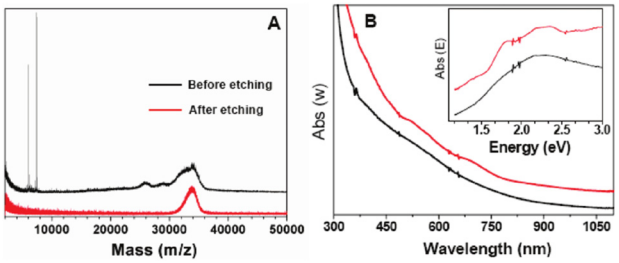

Fig. 4 (A) MALDI mass spectra of Au nanoparticles before (black profile) and after thiol etching and (B). UV-vis absorption spectra of Au nanoparticles before and after thiol etching (inset: optical absorbance *vs.* photon energy). Reproduced with permission from ref. 232. Copyright 2009, American Chemical Society.

6. Solid phase synthesis

It is important to note as well that almost all methods of synthesizing ultra-small metal nanoclusters capped with hydrophobic and hydrophilic ligands are carried out in solution (aqueous or organic phase) but not in the solid phase because interactions between the chemical reactants are more active and more complete. In contrast to the methods mentioned above that are related to solutions, the synthetic method reviewed in this subsection is the solid phase synthesis which contains many merits such as simple operation and large-scale, and this method is widely used to prepare atomically precise highly stable metal nanoclusters.[2] In 2010, Pradeep and coworkers developed a new method (later named the solid state route) to prepare mercaptosuccinic acid (H_2MSA) protected Ag nanoclusters containing nine atoms.[233] The reported synthetic route in this work includes three steps: first of all, by grinding a mixture of silver salt ($AgNO_3$) and a capping agent (H_2MSA) in the solid state in a mortar, polymeric silver–thiolates were prepared using the strong affinity of the sulfur from the capping agent to the metal atom. Second, sodium borohydride (powder state) as a strong reducing agent was added and the polymeric precursor was reduced in the grinding process under a strongly reducing environment, giving birth to the formation of a brownish-black powder. In the last step, a certain amount of pure water was added to complete the reaction, resulting in the formation of strong photoluminescent Ag_9 nanoclusters. Multiple techniques such as XPS, MS and TEM were performed to characterize the as-obtained nanoclusters after their purification using ethanol precipitation, centrifugation and re-extraction

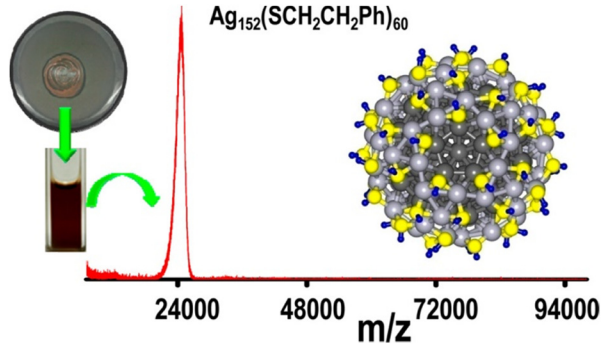

Fig. 5 MALDI mass spectra and optimized structure of the Ag_{152} nanoclusters prepared by a solid state route. Reproduced with permission from ref. 234. Copyright 2012, American Chemical Society.

processes. Chakraborty *et al.* from the same group prepared 2-phenylethanthiol (PET) protected Ag_{152} nanoclusters using a derivative method of the solid state synthesis (Fig. 5).[234] In this synthesis process, ethanol was added in the last step rather than pure water. This small change will benefit the control of the target nanocluster size and cleaning of the final products. Additionally, many atomically precise metal nanoclusters were prepared using this method.[235,236]

7. Intercluster reaction

The reaction between different clusters is proved to be an efficient strategy to prepare multi-metallic nanoclusters. As an emerging method, it is defined as the intercluster reaction. Pradeep's group systemically demonstrated the intercluster reaction between mono-gold and mono-silver clusters, $Au_{25}(PET)_{18}^{-}$ (PET = phenylethanethiolate)[113] and $Ag_{44}(FTP)_{30}^{4-}$ (FTP = 4-fluorothiophenol),[237,238] which gave birth to the formation of bimetallic nanoclusters including silver-doped Au_{25} ($Ag_xAu_{25-x}(SR)_{18}$) and gold-doped Ag_{44} ($Au_xAg_{25-x}(SR)_{18}$) bimetallic nanoclusters (Fig. 6).[239] Interestingly, both parent clusters could spontaneously react in the solvent to exchange the metal atoms as well as the metal–thiolate fragments under ambient conditions. The number of exchanged intermediate species could be controlled by varying the Ag_{44} : Au_{25} molar ratios. In particular, the number of doped silver and gold atoms in the parent clusters could be varied from one atom to 24. In the case of gold-doped

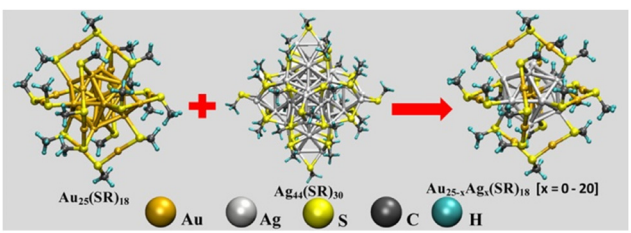

Fig. 6 (a) Schematic illustration of intercluster reactions of Au_{25} and Ag_{44}. Reproduced with permission from ref. 239. Copyright 2016, American Chemical Society.

Ag_{44} clusters, DFT simulations showed that the gold atom preferred to occupy the icosahedral kernel followed by the outer staple motifs and last the second inner dodecahedron, which was confirmed by the bimetallic $Ag_{32}Au_{12}(SR)_{30}$ cluster formed by the substitution of all of the silver atoms in the icosahedral kernel of the Ag_{44} cluster. Besides, using three model monolayer-capped bimetallic nanoclusters, $Ag_{25-x}Au_x(SR)_{18}$, $Au_{25-x}Ag_x(SR)_{18}$, and $Au_xAg_{44-x}(SR)_{30}$, the structure–reactivity correlation in metal atom substitutions was demonstrated and the results showed that although the alloy clusters possessed certain common structural features, they exhibited distinctly different reactivities in the substitution reactions. In detail, the metal atoms at the outermost shells (gold atoms in the $M_2(SR)_3$ motifs of $Ag_{25-x}Au_x(SR)_{18}$ and $Au_xAg_{44-x}(SR)_{30}$, and silver atoms in the $M_2(SR)_5$ motifs of $Au_{25-x}Ag_x(SR)_{18}$) were substituted more easily compared to those at the inner icosahedral sites, and the gold atoms in the second shells of the $Ag_{25-x}Au_x$ nanocluster could be completely replaced by silver atoms, but such complete substitution was not possible for the $Au_{25-x}Ag_x$ cluster. Interestingly, a dianionic adduct, formed in the spontaneous alloying between the two clusters ($Ag_{25}(SR)_{18}$ and $Au_{25}(SR)_{18}$), was detected to be one of the earliest intermediates in the intercluster reaction, suggesting that aside from the fragments, clusters themselves might be involved in the inter-cluster reactions. Coupled with molecular docking simulations, DFT calculations showed that van der Waals forces and bonding between the staple motifs on the periphery of the clusters could be the key factors to form these unique adducts. In addition, a novel $Au_{22}Ir_3(PET)_{18}$ cluster, as the first case of an Ir atom doped monolayer-capped bimetallic cluster, was prepared by Bhat *et al. via* the reaction between $Au_{25}(PET)_{18}$ and $Ir_9(PET)_6$ clusters.[240] Compared to the intermediate products of other intercluster reactions, this reaction formed only one single product, which could be further purified and separated using the thin-layer chromatography (TLC) method and characterized by the ESI-MS and UV-vis techniques. The most favorable geometric structure was calculated with aid of DFT simulations, and the results showed that the alloy cluster possessed a similar skeleton to the Au_{25} cluster, in which one Ir atom was located at the center of the icosahedral kernel and the remaining two Ir atoms were positioned on the icosahedral shell, forming a triangular structure *via* strong Ir–Ir interactions. Khatun and coworkers discussed the intercluster reaction between the bimetallic alloy cluster $MAg_{28}(PPh_3)_4(BDT)_{12}$ (M = Ni, Pt, Pd) and $Au_{25}(PET)_{18}$ cluster, leading to the formation of trimetallic $MAu_xAg_{28-x}(PPh_3)_4(BDT)_{12}$ (x = 1–12).[241] In this reaction, only a maximum of twelve gold doped nanoclusters were formed for the bimetallic cluster as a major product, which was obviously different from previous reports of intercluster reactions. The central atom (Ni, Pd, or Pt) could not be transferred from the center position of the bimetallic cluster to the mono-thiolate capped Au_{25} cluster, suggesting that the central metal atom did not participate in the interaction

reaction. Xia and coworkers reported the synthesis of a novel $Au_{20}Ag_5(Capt)_{18}$ cluster by the reaction between the Au_{25} cluster and ultrasmall silver nanoclusters ($Ag_{30}(Capt)_{18}$).[242] By replacing the Ag_{30} cluster with ultrasmall silver nanoparticles, polydisperse products ($Au_{22}Ag_3S_{12}$, $Au_{21}Ag_4S_{12}$, and $Au_{20}Ag_5S_{12}$) were obtained. Besides, copper atoms could be doped into the Au_{25} cluster by means of the intercluster reaction.

8. Summary and outlook

In this review, we summarized the recent progress in the controllable synthesis of ultra-small metal nanoclusters stabilized by surface protecting ligands and systemically classified these methods into several types, including the Brust–Schiffrin method, ligand-exchange, galvanic/anti-galvanic reaction, etching, solid phase synthesis and intercluster reaction. Among them, both the Brust–Schiffrin and ligand exchange methods are the facile and most widely used methods to prepare both single-component and multi-component metal nanoclusters, and the galvanic/anti-galvanic reaction and intercluster reaction methods are suitable for the synthesis of alloy nanoclusters including bimetallic and trimetallic and even multimetallic nanoclusters. Yet, despite substantial progress in thiolated metal nanoclusters (including diverse structures, compositions and applications), some suggestions are outlined in future work on this fascinating field: (i) the expansion of the types of metal clusters. At present, two types of typical metal nanoclusters (mainly gold and silver nanoclusters) are emerging and promising nanomaterials, whose geometric and electronic structures, sizes, surface capping agents and compositions have been extensively studied. Although the development of copper clusters obviously lags behind the gold and silver nanoclusters in terms of the number, structural diversity and the types of synthesis methods, copper clusters have also attracted considerable attention owing to their novel size-dependent properties. To the best of our knowledge, aside from the coinage clusters, other types of clusters, such as Pt, Pd and Ir clusters, also have great potential application in the energy and catalytic fields. Thus, it is greatly important to fully explore the other types of metal nanoclusters with different sizes, structures and compositions. (ii) In-depth understanding of the details of the cluster synthesis process. In many cases, chemists only focus on the final target cluster and the physicochemical properties and structures associated with it, and lose sight of the important formation mechanism and process. So it is no exaggeration to say that the partly meaningful details of the process of cluster synthesis have been a mystery. However, the mechanism of cluster synthesis or assembly is conducive to understanding the structural transformation of metal nanoclusters in specific experiments. Thus, mass spectroscopy techniques (ESI-MS and MALDI-MS) should be carried out to map out the intermediate mixture species before obtaining the final product to gain more information about the assembly or conversion mechanism of metal nanoclusters in solution. (iii) Exploring the cluster-based potential applications. To be honest, the performance of metal nanoclusters is still far from the actual application. Thus, more work should be devoted to developing new and high-performance cluster-based nanomaterials and revealing their structure–application relationships.

Data availability

No primary research results, software or code have been included and no new data were generated or analysed as part of this review.

Conflicts of interest

There are no conflicts to declare.

Acknowledgements

This work was supported by the National Natural Science Foundation of China (22201225), the China Postdoctoral Science Foundation (2023M733539), the XiangJiang Scholars Scheme Program (XJ2023006), the Postdoctoral Researcher Scientific Activity Funding Project in Anhui Province (2023A660), the Scientific Program Funded by the Shaanxi Provincial Education Department (23JK0456), the Scientific and Technological Plan Project of Xi'an Beilin District (GX2310) and the Scientific and Technological Plan Project of Xi'an Science and Technology Bureau (24GXFW0017).

Notes and references

1 R. Jin, C. Zeng, M. Zhou and Y. Chen, Atomically Precise Colloidal Metal Nanoclusters and Nanoparticles: Fundamentals and Opportunities, *Chem. Rev.*, 2016, **116**, 10346–10413.
2 I. Chakraborty and T. Pradeep, Atomically Precise Clusters of Noble Metals: Emerging Link between Atoms and Nanoparticles, *Chem. Rev.*, 2017, **117**, 8208–8271.
3 A. W. Cook and T. W. Hayton, Case Studies in Nanocluster Synthesis and Characterization: Challenges and Opportunities, *Acc. Chem. Res.*, 2018, **51**, 2456–2464.
4 S. E. Crawford, M. J. Hartmann and J. E. Millstone, Surface Chemistry-Mediated Near-Infrared Emission of Small Coinage Metal Nanoparticles, *Acc. Chem. Res.*, 2019, **52**, 695–703.
5 Q.-M. Wang, Y.-M. Lin and K.-G. Liu, Role of Anions Associated with the Formation and Properties of Silver Clusters, *Acc. Chem. Res.*, 2015, **48**, 1570–1579.
6 A. C. Templeton, W. P. Wuelfing and R. W. Murray, Monolayer-Protected Cluster Molecules, *Acc. Chem. Res.*, 2000, **33**, 27–36.
7 A. Heuer-Jungemann, N. Feliu, I. Bakaimi, M. Hamaly, A. Alkilany, I. Chakraborty, A. Masood, M. F. Casula, A. Kostopoulou, E. Oh, K. Susumu, M. H. Stewart, I. L. Medintz, E. Stratakis, W. J. Parak and A. G. Kanaras, The Role of Ligands in the Chemical Synthesis and Applications of Inorganic Nanoparticles, *Chem. Rev.*, 2019, **119**, 4819–4880.

8 N. Xia and Z. Wu, Controlling ultrasmall gold nanoparticles with atomic precision, *Chem. Sci.*, 2021, **12**, 2368–2380.
9 B. Bhattarai, Y. Zaker, A. Atnagulov, B. Yoon, U. Landman and T. P. Bigioni, Chemistry and Structure of Silver Molecular Nanoparticles, *Acc. Chem. Res.*, 2018, **51**, 3104–3113.
10 S. Sharma, K. K. Chakrahari, J.-Y. Saillard and C. W. Liu, Structurally Precise Dichalcogenolate-Protected Copper and Silver Superatomic Nanoclusters and Their Alloys, *Acc. Chem. Res.*, 2018, **51**, 2475–2483.
11 Y. M. Su, Z. Wang, C. H. Tung, D. Sun and S. Schein, Keplerate Ag_{192} Cluster with 6 Silver and 14 Chalcogenide Octahedral and Tetrahedral Shells, *J. Am. Chem. Soc.*, 2021, **143**, 13235–13244.
12 S. Knoppe and T. Bürgi, Chirality in Thiolate-Protected Gold Clusters, *Acc. Chem. Res.*, 2014, **47**, 1318–1326.
13 M. Agrachev, M. Ruzzi, A. Venzo and F. Maran, Nuclear and Electron Magnetic Resonance Spectroscopies of Atomically Precise Gold Nanoclusters, *Acc. Chem. Res.*, 2019, **52**, 44–52.
14 C. M. Aikens, Electronic and Geometric Structure, Optical Properties, and Excited State Behavior in Atomically Precise Thiolate-Stabilized Noble Metal Nanoclusters, *Acc. Chem. Res.*, 2018, **51**, 3065–3073.
15 M. Hesari and Z. Ding, A Grand Avenue to Au Nanocluster Electrochemiluminescence, *Acc. Chem. Res.*, 2017, **50**, 218–230.
16 K. Kwak and D. Lee, Electrochemistry of Atomically Precise Metal Nanoclusters, *Acc. Chem. Res.*, 2019, **52**, 12–22.
17 B. Nieto-Ortega and T. Bürgi, Vibrational Properties of Thiolate-Protected Gold Nanoclusters, *Acc. Chem. Res.*, 2018, **51**, 2811–2819.
18 Q. Tang, G. Hu, V. Fung and D.-e. Jiang, Insights into Interfaces, Stability, Electronic Properties, and Catalytic Activities of Atomically Precise Metal Nanoclusters from First Principles, *Acc. Chem. Res.*, 2018, **51**, 2793–2802.
19 Z. Liu, Y. Li, E. Kahng, S. Xue, X. Du, S. Li and R. Jin, Tailoring the Electron-Phonon Interaction in Au25(SR)18 Nanoclusters via Ligand Engineering and Insight into Luminescence, *ACS Nano*, 2022, **16**, 18448–18458.
20 G. Deng, S. Malola, J. Yan, Y. Han, P. Yuan, C. Zhao, X. Yuan, S. Lin, Z. Tang, B. K. Teo, H. Hakkinen and N. Zheng, From Symmetry Breaking to Unraveling the Origin of the Chirality of Ligated $Au_{13}Cu_2$ Nanoclusters, *Angew. Chem., Int. Ed.*, 2018, **57**, 3421–3425.
21 S. Tian, Y. Z. Li, M. B. Li, J. Yuan, J. Yang, Z. Wu and R. Jin, Structural isomerism in gold nanoparticles revealed by X-ray crystallography, *Nat. Commun.*, 2015, **6**, 8667.
22 S. Wang, X. Meng, A. Das, T. Li, Y. Song, T. Cao, X. Zhu, M. Zhu and R. Jin, A 200-fold quantum yield boost in the photoluminescence of silver-doped Ag_xAu_{25-x} nanoclusters: the 13th silver atom matters, *Angew. Chem., Int. Ed.*, 2014, **53**(9), 2376–2380.
23 Z.-J. Guan, F. Hu, J.-J. Li, Z.-R. Wen, Y.-M. Lin and Q.-M. Wang, Isomerization in Alkynyl-Protected Gold Nanoclusters, *J. Am. Chem. Soc.*, 2020, **142**, 2995–3001.
24 B. Yin, L. R. Jiang, X. J. Wang, Y. Liu, K. Y. Kuang, M. M. Jing, C. M. Fang, C. J. Zhou, S. Chen and M. Z. Zhu, Bright dual-color electrochemiluminescence of a structurally determined Pt_1Ag_{18} nanocluster, *Aggregate*, 2024, **5**, e417.
25 Z. Wang, J.-W. Liu, H.-F. Su, Q.-Q. Zhao, M. Kurmoo, X.-P. Wang, C.-H. Tung, D. Sun and L.-S. Zheng, Chalcogens-Induced $Ag_6Z_4@Ag_{36}$ (Z = S or Se) Core-Shell Nanoclusters: Enlarged Tetrahedral Core and Homochiral Crystallization, *J. Am. Chem. Soc.*, 2019, **141**, 17884–17890.
26 Y. M. Su, Z. Wang, S. Schein, C. H. Tung and D. Sun, A Keplerian Ag_{90} nest of Platonic and Archimedean polyhedra in different symmetry groups, *Nat. Commun.*, 2020, **11**, 3316.
27 W.-Q. Shi, L. Zeng, R.-L. He, X.-S. Han, Z.-J. Guan, M. Zhou and Q.-M. Wang, Near-unity NIR phosphorescent quantum yield from a room-temperature solvated metal nanocluster, *Science*, 2024, **383**, 326–330.
28 Y. Zhu, H. Qian, M. Zhu and R. Jin, Thiolate-Protected Aun Nanoclusters as Catalysts for Selective Oxidation and Hydrogenation Processes, *Adv. Mater.*, 2010, **22**, 1915–1920.
29 X.-D. Zhang, Z. Luo, J. Chen, X. Shen, S. Song, Y. Sun, S. Fan, F. Fan, D. T. Leong and J. Xie, Ultrasmall $Au_{10\text{-}12}(SG)_{10\text{-}12}$ nanomolecules for high tumor specificity and cancer radiotherapy, *Adv. Mater.*, 2014, **26**, 4565.
30 X. Yuan, Z. Luo, Y. Yu, Q. Yao and J. Xie, Luminescent Noble Metal Nanoclusters as an Emerging Optical Probe for Sensor Development, *Chem. – Asian J.*, 2013, **8**, 858–871.
31 D. Yang, W. Pei, S. Zhou, J. Zhao, W. Ding and Y. Zhu, Controllable Conversion of CO_2 on Non-metallic Gold Clusters, *Angew. Chem., Int. Ed.*, 2020, **59**, 1919–1924.
32 H. Peng, Z. Huang, Y. Sheng, X. Zhang, H. Deng, W. Chen and J. Liu, Pre-oxidation of Gold Nanoclusters Results in a 66 % Anodic Electrochemiluminescence Yield and Drives Mechanistic Insights, *Angew. Chem., Int. Ed.*, 2019, **58**, 11691–11694.
33 M. Miyauchi, H. Irie, M. Liu, X. Q. Qiu, H. G. Yu, K. Sunada and K. Hashimoto, Visible-Light-Sensitive Photocatalysts: Nanocluster-Grafted Titanium Dioxide for Indoor Environmental Remediation, *J. Phys. Chem. Lett.*, 2016, **7**, 75–84.
34 Y. Lu, C. Zhang, X. Li, A. R. Frojd, W. Xing, A. Z. Clayborne and W. Chen, Significantly enhanced electrocatalytic activity of Au_{25} clusters by single platinum atom doping, *Nano Energy*, 2018, **50**, 316–322.
35 H. Liu, G. Hong, Z. Luo, J. Chen, J. Chang, M. Gong, H. He, J. Yang, X. Yuan, L. Li, X. Mu, J. Wang, W. Mi, J. Luo, J. Xie and X.-D. Zhang, Atomic-Precision Gold Clusters for NIR-II Imaging, *Adv. Mater.*, 2019, **31**, 1901015.
36 Y. Chen, M. L. Phipps, J. H. Werner, S. Chakraborty and J. S. Martinez, DNA Templated Metal Nanoclusters: From Emergent Properties to Unique Applications, *Acc. Chem. Res.*, 2018, **51**, 2756–2763.
37 M. A. Hewitt, H. Hernandez and G. E. Johnson, Light Exposure Promotes Degradation of Intermediates and Growth of Phosphine-Ligated Gold Clusters, *J. Phys. Chem. C*, 2020, **124**, 3396–3402.

38 C. Deng, C. Sun, Z. Wang, Y. Tao, Y. Chen, J. Lin, G. Luo, B. Lin, D. Sun and L. Zheng, A Sodalite-Type Silver Orthophosphate Cluster in a Globular Silver Nanocluster, *Angew. Chem., Int. Ed.*, 2020, **59**, 12659–12663.

39 H. Zhao, C. Zhang, B. Han, Z. Wang, Y. Liu, Q. Xue, C.-H. Tung and D. Sun, Templated synthesis of high nuclearity Cu(I) alkynide nanoclusters at room temperature, *Nat. Synth.*, 2024, **3**, 517–526.

40 X. J. Wang, B. Yin, L. R. Jiang, C. Yang, Y. Liu, G. Zou, S. Chen and M. Z. Zhu, Ligand-protected metal nanoclusters as low-loss, highly polarized emitters for optical waveguides, *Science*, 2023, **381**, 784–790.

41 L. Liu, S. J. Zheng, H. Chen, J. M. Cai and S. Q. Zang, Tandem Nitrate-to-Ammonia Conversion on Atomically Precise Silver Nanocluster/MXene Electrocatalyst, *Angew. Chem., Int. Ed.*, 2024, **63**, e202316910.

42 X. Kang, S. Jin, L. Xiong, X. Wei, M. Zhou, C. Qin, Y. Pei, S. Wang and M. Zhu, Nanocluster growth via "graft-onto": effects on geometric structures and optical properties, *Chem. Sci.*, 2020, **11**, 1691–1697.

43 C.-Q. Jiao, C.-Y. Duan, J.-X. Hu, J.-L. Wang, L. Zhao, W. Wen, W.-J. Jiang, Y.-S. Meng, T. Liu and G. G. Gurzadyan, Manipulation of successive crystalline transformations to control electron transfer and switchable functions, *Natl. Sci. Rev.*, 2018, **5**, 507–515.

44 Z. Gan, J. Chen, J. Wang, C. Wang, M. B. Li, C. Yao, S. Zhuang, A. Xu, L. Li and Z. Wu, The fourth crystallographic closest packing unveiled in the gold nanocluster crystal, *Nat. Commun.*, 2017, **8**, 14739.

45 L. He, J. Yuan, N. Xia, L. Liao, X. Liu, Z. Gan, C. Wang, J. Yang and Z. Wu, Kernel Tuning and Nonuniform Influence on Optical and Electrochemical Gaps of Bimetal Nanoclusters, *J. Am. Chem. Soc.*, 2018, **140**, 3487–3490.

46 Y. Chen, C. Liu, Q. Tang, C. Zeng, T. Higaki, A. Das, D.-e. Jiang, N. L. Rosi and R. Jin, Isomerism in $Au_{28}(SR)_{20}$Nanocluster and Stable Structures, *J. Am. Chem. Soc.*, 2016, **138**, 1482–1485.

47 A. K. Das, S. Biswas, V. S. Wani, A. S. Nair, B. Pathak and S. Mandal, $[Cu_{18}H_3(S\text{-}Adm)_{12}(PPh_3)_4Cl_2]$: fusion of Platonic and Johnson solids through a Cu(0) center and its photophysical properties, *Chem. Sci.*, 2022, **13**, 7616–7625.

48 H. Dong, L. Liao and Z. Wu, Two-Way Transformation between fcc- and Nonfcc-Structured Gold Nanoclusters, *J. Phys. Chem. Lett.*, 2017, 5338–5343.

49 W. Du, S. Jin, L. Xiong, M. Chen, J. Zhang, X. Zou, Y. Pei, S. Wang and M. Zhu, $Ag_{50}(Dppm)_6(SR)_{30}$ and Its Homologue $Au_xAg_{50-x}(Dppm)_6(SR)_{30}$ Alloy Nanocluster: Seeded Growth, Structure Determination, and Differences in Properties, *J. Am. Chem. Soc.*, 2017, **139**, 1618–1624.

50 T. Higaki, C. Zeng, Y. Chen, E. Hussain and R. Jin, Controlling the crystalline phases (FCC, HCP and BCC) of thiolate-protected gold nanoclusters by ligand-based strategies, *CrystEngComm*, 2016, **18**, 6979–6986.

51 Q. Li, T. Y. Luo, M. G. Taylor, S. X. Wang, X. F. Zhu, Y. B. Song, G. Mpourmpakis, N. L. Rosi and R. C. Jin, Molecular "surgery" on a 23-gold-atom nanoparticle, *Sci. Adv.*, 2017, **3**, e1603193.

52 L. He, X. He, J. Wang, C. Fu and J. Liang, $Ag_{23}Au_2$ and $Ag_{22}Au_3$: A Model of Cocrystallization in Bimetal Nanoclusters, *Inorg. Chem.*, 2021, **60**, 8404–8408.

53 Y. Zhou, W. M. Gu, R. G. Wang, W. L. Zhu, Z. Y. Hu, W. W. Fei, S. L. Zhuang, J. Li, H. T. Deng, N. Xia, J. He and Z. K. Wu, Controlled Sequential Doping of Metal Nanocluster, *Nano Lett.*, 2024, **24**, 2226–2233.

54 L. Liao, S. Zhou, Y. Dai, L. Liu, C. Yao, C. Fu, J. Yang and Z. Wu, Mono-Mercury Doping of Au_{25} and the HOMO/LUMO Energies Evaluation Employing Differential Pulse Voltammetry, *J. Am. Chem. Soc.*, 2015, **137**, 9511–9514.

55 X. Yuan, Z. Luo, Q. Zhang, X. Zhang, Y. Zheng, J. Y. Lee and J. Xie, Synthesis of Highly Fluorescent Metal (Ag, Au, Pt, and Cu) Nanoclusters by Electrostatically Induced Reversible Phase Transfer, *ACS Nano*, 2011, **5**, 8800–8808.

56 S. Hossain, D. Suzuki, T. Iwasa, R. Kaneko, T. Suzuki, S. Miyajima, Y. Iwamatsu, S. Pollitt, T. Kawawaki, N. Barrabés, G. Rupprechter and Y. Negishi, Determining and Controlling Cu-Substitution Sites in Thiolate-Protected Gold-Based 25-Atom Alloy Nanoclusters, *J. Phys. Chem. C*, 2020, **124**, 22304–22313.

57 S. Hossain, Y. Niihori, L. V. Nair, B. Kumar, W. Kurashige and Y. Negishi, Alloy Clusters: Precise Synthesis and Mixing Effects, *Acc. Chem. Res.*, 2018, **51**, 3114–3124.

58 T. Higaki, Q. Li, M. Zhou, S. Zhao, Y. Li, S. Li and R. Jin, Toward the Tailoring Chemistry of Metal Nanoclusters for Enhancing Functionalities, *Acc. Chem. Res.*, 2018, **51**, 2764–2773.

59 M. S. Bootharaju, C. P. Joshi, M. R. Parida, O. F. Mohammed and O. M. Bakr, Templated Atom-Precise Galvanic Synthesis and Structure Elucidation of a $[Ag_{24}Au(SR)_{18}]^-$ Nanocluster, *Angew. Chem., Int. Ed.*, 2016, **55**, 922–926.

60 W. T. Chang, S. Sharma, J. H. Liao, S. Kahlal, Y. C. Liu, M. H. Chiang, J. Y. Saillard and C. W. Liu, Heteroatom-Doping Increases Cluster Nuclearity: From an $[Ag_{20}]$ to an $[Au_3Ag_{18}]$ Core, *Chem. – Eur. J.*, 2018, **24**, 14352–14357.

61 Z. Chen, A. G. Walsh, X. Wei, M. Zhu and P. Zhang, New Insights into the Bonding Properties of $[Ag_{25}(SR)_{18}]^-$ Nanoclusters from X-ray Absorption Spectroscopy, *J. Phys. Chem. C*, 2022, **126**, 12721–12727.

62 S. Jin, M. Zhou, X. Kang, X. Li, W. Du, X. Wei, S. Chen, S. Wang and M. Zhu, Three-dimensional Octameric Assembly of Icosahedral M13 Units in $[Au_8Ag_{57}(Dppp)_4(C_6H_{11}S)_{32}Cl_2]Cl$ and its $[Au_8Ag_{55}(Dppp)_4(C_6H_{11}S)_{34}][BPh_4]_2$ Derivative, *Angew. Chem., Int. Ed.*, 2020, **59**, 3891–3895.

63 X. Kang, X. Wei, S. Jin, Q. Yuan, X. Luan, Y. Pei, S. Wang, M. Zhu and R. Jin, Rational construction of a library of M_{29} nanoclusters from monometallic to tetrametallic, *Proc. Natl. Acad. Sci. U. S. A.*, 2019, **116**, 18834–18840.

64 K. Zheng and J. Xie, Composition-Dependent Antimicrobial Ability of Full-Spectrum Au_xAg_{25-x} Alloy Nanoclusters, *ACS Nano*, 2020, **14**, 11533–11541.

65 X. Zou, S. He, X. Kang, S. Chen, H. Yu, S. Jin, D. Astruc and M. Zhu, New atomically precise M_1Ag_{21} (M = Au/Ag)

nanoclusters as excellent oxygen reduction reaction catalysts, *Chem. Sci.*, 2021, **12**, 3660–3667.

66 X. Liu, J. Yuan, C. Yao, J. Chen, L. Li, X. Bao, J. Yang and Z. Wu, Crystal and Solution Photoluminescence of $MAg_{24}(SR)_{18}$ (M = Ag/Pd/Pt/Au) Nanoclusters and Some Implications for the Photoluminescence Mechanisms, *J. Phys. Chem. C*, 2017, **121**, 13848–13853.

67 L. G. AbdulHalim, Z. Hooshmand, M. R. Parida, S. M. Aly, D. Le, X. Zhang, T. S. Rahman, M. Pelton, Y. Losovyj, P. A. Dowben, O. M. Bakr, O. F. Mohammed and K. Katsiev, pH-Induced Surface Modification of Atomically Precise Silver Nanoclusters: An Approach for Tunable Optical and Electronic Properties, *Inorg. Chem.*, 2016, **55**, 11522–11528.

68 B. D. Cox, P. H. Woodworth, P. D. Wilkerson, M. F. Bertino and J. E. Reiner, Ligand-Induced Structural Changes of Thiolate-Capped Gold Nanoclusters Observed with Resistive-Pulse Nanopore Sensing, *J. Am. Chem. Soc.*, 2019, **141**, 3792–3796.

69 Z.-J. Guan, R.-L. He, S.-F. Yuan, J.-J. Li, F. Hu, C.-Y. Liu and Q.-M. Wang, Ligand Engineering toward the Trade-Off between Stability and Activity in Cluster Catalysis, *Angew. Chem., Int. Ed.*, 2022, **61**, e202116965.

70 T. Kawawaki, A. Ebina, Y. Hosokawa, S. Ozaki, D. Suzuki, S. Hossain and Y. Negishi, Thiolate-Protected Metal Nanoclusters: Recent Development in Synthesis, Understanding of Reaction, and Application in Energy and Environmental Field, *Small*, 2021, **17**, 2005328.

71 X. Ma, Y. Lv, H. Li, T. Chen, J. Zeng, M. Zhu and H. Yu, Ligand Effect on Geometry and Electronic Structures of Face-Centered Cubic Ag_{14} and Ag_{23} Nanoclusters, *J. Phys. Chem. C*, 2020, **124**, 13421–13426.

72 Q. Xue, Z. Wang, S. Han, Y. Liu, X. Dou, Y. Li, H. Zhu and X. Yuan, Ligand engineering of Au nanoclusters with multifunctional metalloporphyrins for photocatalytic H2O2 production, *J. Mater. Chem. A*, 2022, **10**, 8371–8377.

73 J. Yan, B. K. Teo and N. Zheng, Surface Chemistry of Atomically Precise Coinage-Metal Nanoclusters: From Structural Control to Surface Reactivity and Catalysis, *Acc. Chem. Res.*, 2018, **51**, 3084–3093.

74 D. Eguchi, M. Sakamoto and T. Teranishi, Ligand effect on the catalytic activity of porphyrin-protected gold clusters in the electrochemical hydrogen evolution reaction, *Chem. Sci.*, 2018, **9**, 261–265.

75 D. M. Chevrier, L. Raich, C. Rovira, A. Das, Z. Luo, Q. Yao, A. Chatt, J. Xie, R. Jin, J. Akola and P. Zhang, Molecular-Scale Ligand Effects in Small Gold-Thiolate Nanoclusters, *J. Am. Chem. Soc.*, 2018, **140**, 15430–15436.

76 A. Cirri, H. M. Hernández and C. J. Johnson, chloride, and bromide show similar electronic effects in the $Au_9(PPh_3)_8^{3+}$ nanocluster, *Chem. Commun.*, 2020, **56**, 1283–1285.

77 Z. Gan, N. Xia, N. Yan, S. Zhuang, J. Dong, Y. Zhao, S. Jiang, Q. Tao and Z. Wu, Compression-Driven Internanocluster Reaction for Synthesis of Unconventional Gold Nanoclusters, *Angew. Chem., Int. Ed.*, 2021, **60**, 12253–12257.

78 T.-H. Huang, F.-Z. Zhao, Q.-L. Hu, Q. Liu, T.-C. Wu, D. Zheng, T. Kang, L.-C. Gui and J. Chen, Bisphosphine-Stabilized Gold Nanoclusters with the Crown/Birdcage-Shaped Au_{11} Cores: Structures and Optical Properties, *Inorg. Chem.*, 2020, **59**, 16027–16034.

79 K. R. Krishnadas, G. Natarajan, A. Baksi, A. Ghosh, E. Khatun and T. Pradeep, Metal-Ligand Interface in the Chemical Reactions of Ligand-Protected Noble Metal Clusters, *Langmuir*, 2019, **35**, 11243–11254.

80 B. Kumar, T. Kawawaki, N. Shimizu, Y. Imai, D. Suzuki, S. Hossain, L. V. Nair and Y. Negishi, Gold nanoclusters as electrocatalysts: size, ligands, heteroatom doping, and charge dependences, *Nanoscale*, 2020, **12**, 9969–9979.

81 S. Li, A. V. Nagarajan, D. R. Alfonso, M. Sun, D. R. Kauffman, G. Mpourmpakis and R. Jin, Boosting CO2 Electrochemical Reduction with Atomically Precise Surface Modification on Gold Nanoclusters, *Angew. Chem., Int. Ed.*, 2021, **60**, 6351–6356.

82 Y. Li and R. Jin, Seeing Ligands on Nanoclusters and in Their Assemblies by X-ray Crystallography: Atomically Precise Nanochemistry and Beyond, *J. Am. Chem. Soc.*, 2020, **142**, 13627–13644.

83 Y. Lin, P. Charchar, A. J. Christofferson, M. R. Thomas, N. Todorova, M. M. Mazo, Q. Chen, J. Doutch, R. Richardson, I. Yarovsky and M. M. Stevens, Surface Dynamics and Ligand-Core Interactions of Quantum Sized Photoluminescent Gold Nanoclusters, *J. Am. Chem. Soc.*, 2018, **140**, 18217–18226.

84 S. Li, Y. Sun, C. Wu, W. Hu, W. Li, X. Liu, M. Chen and Y. Zhu, Distinct structure assembly driven by metal–ligand binding in Au_{23} nanoclusters and its relation to photocatalysis, *Chem. Commun.*, 2021, **57**, 2176–2179.

85 Y. Li, M. J. Cowan, M. Zhou, T.-Y. Luo, Y. Song, H. Wang, N. L. Rosi, G. Mpourmpakis and R. Jin, Atom-by-Atom Evolution of the Same Ligand-Protected Au_{21}, Au_{22}, Au_{22}-Cd_1, and Au_{24} Nanocluster Series, *J. Am. Chem. Soc.*, 2020, **142**, 20426–20433.

86 J. Yagi, A. Ikeda, L.-C. Wang, C.-S. Yeh and H. Kawasaki, Singlet Oxygen Generation Using Thiolated Gold Nanoclusters under Photo- and Ultrasonic Excitation: Size and Ligand Effect, *J. Phys. Chem. C*, 2022, **126**, 19693–19704.

87 J. Xu, L. Xiong, X. Cai, S. Tang, A. Tang, X. Liu, Y. Pei and Y. Zhu, Evolution from superatomic $Au_{24}Ag_{20}$ monomers into molecular-like $Au_{43}Ag_{38}$ dimeric nanoclusters, *Chem. Sci.*, 2022, **13**, 2778–2782.

88 L. Luo, Z. Liu, X. Du and R. Jin, Near-Infrared Dual Emission from the $Au_{42}(SR)_{32}$ Nanocluster and Tailoring of Intersystem Crossing, *J. Am. Chem. Soc.*, 2022, **144**, 19243–19247.

89 J. J. Li, Z. Liu, Z. J. Guan, X. S. Han, W. Q. Shi and Q. M. Wang, A 59-Electron Non-Magic-Number Gold Nanocluster $Au_{99}(C{\equiv}CR)_{40}$ Showing Unexpectedly High Stability, *J. Am. Chem. Soc.*, 2022, **144**, 690–694.

90 H. Li, C. Zhou, E. Wang, X. Kang, W. W. Xu and M. Zhu, An insight, at the atomic level, into the intramolecular metallophilic interaction in nanoclusters, *Chem. Commun.*, 2022, **58**, 5092–5095.

91 Z.-H. Gao, K. Wei, T. Wu, J. Dong, D.-E. Jiang, S. Sun and L.-S. Wang, A Heteroleptic Gold Hydride Nanocluster for Efficient and Selective Electrocatalytic Reduction of CO_2 to CO, *J. Am. Chem. Soc.*, 2022, **144**, 5258–5262.

92 Q. Zhu, X. Huang, Y. Zeng, K. Sun, L. Zhou, Y. Liu, L. Luo, S. Tian and X. Sun, Controllable synthesis and electrocatalytic applications of atomically precise gold nanoclusters, *Nanoscale Adv.*, 2021, **3**, 6330–6341.

93 L. Xu, Q. Li, T. Li, J. Chai, S. Yang and M. Zhu, Construction of a new $Au_{27}Cd_1(SAdm)_{14}(DPPF)Cl$ nanocluster by surface engineering and insight into its structure-property correlation, *Inorg. Chem. Front.*, 2021, **8**, 4820–4827.

94 Y. Du, H. Sheng, D. Astruc and M. Zhu, Atomically Precise Noble Metal Nanoclusters as Efficient Catalysts: A Bridge between Structure and Properties, *Chem. Rev.*, 2020, **120**, 526–622.

95 Y. Jin, C. Zhang, X.-Y. Dong, S.-Q. Zang and T. C. W. Mak, Shell engineering to achieve modification and assembly of atomically-precise silver clusters, *Chem. Soc. Rev.*, 2021, **50**, 2297–2319.

96 X. Kang, Y. Li, M. Zhu and R. Jin, Atomically precise alloy nanoclusters: syntheses, structures, and properties, *Chem. Soc. Rev.*, 2020, **49**, 6443–6514.

97 W. Kurashige, Y. Niihori, S. Sharma and Y. Negishi, Precise synthesis, functionalization and application of thiolate-protected gold clusters, *Coord. Chem. Rev.*, 2016, **320-321**, 238–250.

98 Z. Wang, X. Pan, S. Qian, G. Yang, F. Du and X. Yuan, The beauty of binary phases: A facile strategy for synthesis, processing, functionalization, and application of ultrasmall metal nanoclusters, *Coord. Chem. Rev.*, 2021, **438**, 213900.

99 R. R. Nasaruddin, T. Chen, N. Yan and J. Xie, Roles of thiolate ligands in the synthesis, properties and catalytic application of gold nanoclusters, *Coord. Chem. Rev.*, 2018, **368**, 60–79.

100 C. Sun, B. K. Teo, C. Deng, J. Lin, G.-G. Luo, C.-H. Tung and D. Sun, Hydrido-coinage-metal clusters: Rational design, synthetic protocols and structural characteristics, *Coord. Chem. Rev.*, 2021, **427**, 213576.

101 M. Brust, M. Walker, D. Bethell, D. J. Schiffrin and R. Whyman, Synthesis of Thiol-derivatised Gold Nanoparticles in a Two-phase Liquid-Liquid System, *J. Chem. Soc., Chem. Commun.*, 1994, 801–802.

102 R. L. Donkers, D. Lee and R. W. Murray, Synthesis and Isolation of the Molecule-like Cluster $Au_{38}(PhCH_2CH_2S)_{24}$, *Langmuir*, 2004, **20**, 1945–1952.

103 Y. Li, O. Zaluzhna, B. Xu, Y. Gao, J. M. Modest and Y. J. Tong, Mechanistic Insights into the Brust-Schiffrin Two-Phase Synthesis of Organo-chalcogenate-Protected Metal Nanoparticles, *J. Am. Chem. Soc.*, 2011, **133**, 2092–2095.

104 X. Yuan, Y. Yu, Q. Yao, Q. Zhang and J. Xie, Fast Synthesis of Thiolated Au_{25} Nanoclusters via Protection-Deprotection Method, *J. Phys. Chem. Lett.*, 2012, **3**, 2310–2314.

105 Z. Wu, J. Suhan and R. Jin, One-pot synthesis of atomically monodisperse, thiol-functionalized Au_{25} nanoclusters, *J. Mater. Chem.*, 2009, **19**, 622–626.

106 Z. Wu, E. Lanni, W. Chen, M. E. Bier, D. Ly and R. Jin, High Yield, Large Scale Synthesis of Thiolate-Protected Ag_7 Clusters, *J. Am. Chem. Soc.*, 2009, **131**, 16672–16674.

107 J. F. Parker, J. E. Weaver, F. McCallum, C. A. Fields-Zinna and R. W. Murray, Synthesis of monodisperse $[Oct_4N^+][Au_{25}(SR)_{18}^-]$ nanoparticles, with some mechanistic observations, *Langmuir*, 2010, **26**, 13650–13654.

108 A. Ghosh, T. Udayabhaskararao and T. Pradeep, One-Step Route to Luminescent $Au_{18}SG_{14}$ in the Condensed Phase and Its Closed Shell Molecular Ions in the Gas Phase, *J. Phys. Chem. Lett.*, 2012, **3**, 1997–2002.

109 V. L. Jimenez, D. G. Georganopoulou, R. J. White, A. S. Harper, A. J. Mills, D. Lee and R. W. Murray, Hexanethiolate Monolayer Protected 38 Gold Atom Cluster, *Langmuir*, 2004, **20**, 6864–6870.

110 X. Yuan, L. L. Chng, J. Yang and J. Y. Ying, Miscible-Solvent-Assisted Two-Phase Synthesis of Monolayer-Ligand-Protected Metal Nanoclusters with Various Sizes, *Adv. Mater.*, 2020, **32**, 1906063.

111 S. Chen, A. C. Templeton and R. W. Murray, Monolayer-Protected Cluster Growth Dynamics, *Langmuir*, 2000, **16**, 3543–3548.

112 W. W. Weare, S. M. Reed, M. G. Warner and J. E. Hutchison, *J. Am. Chem. Soc.*, 2000, **122**, 12890–12891.

113 Y. Shichibu, Y. Negishi, T. Tsukuda and T. Teranishi, Large-Scale Synthesis of Thiolated Au_{25} Clusters via Ligand Exchange Reactions of Phosphine-Stabilized Au11 Clusters, *J. Am. Chem. Soc.*, 2005, **127**, 13464–13465.

114 Y. Negishi, N. K. Chaki, Y. Shichibu, R. L. Whetten and T. Tsukuda, Origin of Magic Stability of Thiolated Gold Clusters_ A Case Study on $Au_{25}(SC_6H_{13})_{18}$, *J. Am. Chem. Soc.*, 2007, **129**, 11322–11323.

115 Y. Shichibu, Y. Negishi, T. Watanabe, N. K. Chaki, H. Kawaguchi and T. Tsukuda, Biicosahedral Gold Clusters $[Au_{25}(PPh_3)_{10}(SC_nH_{2n+1})_5Cl_2]^{2+}$ (n = 2-18): A Stepping Stone to Cluster-Assembled Materials, *J. Phys. Chem. C*, 2007, **111**, 7845–7847.

116 J. Akola, M. Walter, R. L. Whetten, H. Häkkinen and H. Grönbeck, On the Structure of Thiolate-Protected Au25, *J. Am. Chem. Soc.*, 2008, **130**, 3756–3757.

117 M. W. Heaven, A. Dass, P. S. White, K. M. Holt and R. W. Murray, Crystal Structure of the Gold Nanoparticle $[N(C_8H_{17})_4][Au_{25}(SCH_2CH_2Ph)_{18}]$, *J. Am. Chem. Soc.*, 2008, **130**, 3754–3755.

118 Z. Wu and R. Jin, Stability of the Two Au-S Binding Modes in $Au_{25}(SG)_{18}$ Nanoclusters Probed by NMR and Optical Spectroscopy, *ACS Nano*, 2009, **3**, 2036.

119 Y. Negishi, W. Kurashige and U. Kamimura, Isolation and Structural Characterization of an Octaneselenolate-Protected Au_{25} Cluster, *Langmuir*, 2011, **27**, 12289–12292.

120 D. R. Kauffman, D. Alfonso, C. Matranga, P. Ohodnicki, X. Deng, R. C. Siva, C. Zeng and R. Jin, Probing active site chemistry with differently charged Au_{25}^q nanoclusters (q = −1, 0, +1), *Chem. Sci.*, 2014, **5**, 3151–3157.

121 Z. Luo, V. Nachammai, B. Zhang, N. Yan, D. T. Leong, D.-e. Jiang and J. Xie, Toward understanding the growth

mechanism: tracing all stable intermediate species from reduction of Au(I)-thiolate complexes to evolution of Au_{25} nanoclusters, *J. Am. Chem. Soc.*, 2014, **136**, 10577–10580.

122 T. Dainese, S. Antonello, J. A. Gascón, F. Pan, N. V. Perera, M. Ruzzi, A. Venzo, A. Zoleo, K. Rissanen and F. Maran, $Au_{25}(SEt)_{18}$, a Nearly Naked Thiolate-Protected Au_{25} Cluster: Structural Analysis by Single Crystal X-ray Crystallography and Electron Nuclear Double Resonance, *ACS Nano*, 2014, **4**, 3904–3912.

123 C. Yao, Y. J. Lin, J. Yuan, L. Liao, M. Zhu, L. H. Weng, J. Yang and Z. Wu, Mono-cadmium vs Mono-mercury Doping of Au_{25} Nanoclusters, *J. Am. Chem. Soc.*, 2015, **137**, 15350–15353.

124 Y. Cao, T. Chen, Q. Yao and J. Xie, Diversification of Metallic Molecules through Derivatization Chemistry of Au_{25} Nanoclusters, *Acc. Chem. Res.*, 2021, **54**, 4142–4153.

125 X. Kang, H. Chong and M. Zhu, $Au_{25}(SR)_{18}$: the captain of the great nanocluster ship, *Nanoscale*, 2018, **10**, 10758–10834.

126 B. Adhikari and A. Banerjee, Facile Synthesis of Water-Soluble Fluorescent Silver Nanoclusters and HgII Sensing, *Chem. Mater.*, 2010, **22**, 4364–4371.

127 G. Li, Z. Lei and Q.-M. Wang, Luminescent Molecular Ag-S Nanocluster $[Ag_{62}S_{13}(SBut)_{32}](BF_4)_4$, *J. Am. Chem. Soc.*, 2010, **132**, 17678–17679.

128 H. Xiang, S.-H. Wei and X. Gong, Structures of $[Ag_7(SR)_4]^-$ and $[Ag_7(DMSA)_4]^-$, *J. Am. Chem. Soc.*, 2010, **132**, 7355–7360.

129 K. M. Harkness, Y. Tang, A. Dass, J. Pan, N. Kothalawala, V. J. Reddy, D. E. Cliffel, B. Demeler, F. Stellacci, O. M. Bakr and J. A. McLean, $Ag_{44}(SR)_{30}^{4-}$: a silver-thiolate superatom complex, *Nanoscale*, 2012, **4**, 4269–4274.

130 H. Yang, Y. Wang, H. Huang, L. Gell, L. Lehtovaara, S. Malola, H. Hakkinen and N. Zheng, All-thiol-stabilized Ag_{44} and $Au_{12}Ag_{32}$ nanoparticles with single-crystal structures, *Nat. Commun.*, 2013, **4**, 2422.

131 L. G. AbdulHalim, M. S. Bootharaju, Q. Tang, S. Del Gobbo, R. G. AbdulHalim, M. Eddaoudi, D. E. Jiang and O. M. Bakr, $Ag_{29}(BDT)_{12}(TPP)_4$: A Tetravalent Nanocluster, *J. Am. Chem. Soc.*, 2015, **137**, 11970–11975.

132 M. Qu, H. Li, L. H. Xie, S. T. Yan, J. R. Li, J. H. Wang, C. Y. Wei, Y. W. Wu and X. M. Zhang, Bidentate Phosphine-Assisted Synthesis of an All-Alkynyl-Protected Ag_{74} Nanocluster, *J. Am. Chem. Soc.*, 2017, **139**, 12346–12349.

133 C. P. Joshi, M. S. Bootharaju, M. J. Alhilaly and O. M. Bakr, $[Ag_{25}(SR)_{18}]^-$: The "Golden" Silver Nanoparticle, *J. Am. Chem. Soc.*, 2015, **137**, 11578–11581.

134 J.-Y. Liu, F. Alkan, Z. Wang, Z.-Y. Zhang, M. Kurmoo, Z. Yan, Q.-Q. Zhao, C. M. Aikens, C.-H. Tung and D. Sun, Different Silver Nanoparticles in One Crystal: $Ag_{210}(^{i}PrPhS)_{71}(Ph_3P)_5Cl$ and $Ag_{211}(^{i}PrPhS)_{71}(Ph_3P)_6Cl$, *Angew. Chem., Int. Ed.*, 2019, **58**, 195–199.

135 F. Hu, J.-J. Li, Z.-J. Guan, S.-F. Yuan and Q.-M. Wang, Formation of an Alkynyl-Protected Ag_{112} Silver Nanocluster as Promoted by Chloride Released In Situ from CH_2Cl_2, *Angew. Chem., Int. Ed.*, 2020, **59**, 5312–5315.

136 P. J. G. Goulet and R. B. Lennox, New Insights into Brust-Schiffrin Metal Nanoparticle Synthesis, *J. Am. Chem. Soc.*, 2010, **132**, 9582–9584.

137 C. A. Fields-Zinna, M. C. Crowe, A. Dass, J. E. Weaver and R. W. Murray, Mass spectrometry of small bimetal monolayer-protected clusters, *Langmuir*, 2009, **25**, 7704–7710.

138 Y. Negishi, T. Iwai and M. Ide, Continuous modulation of electronic structure of stable thiolate-protected Au_{25} cluster by Ag doping, *Chem. Commun.*, 2010, **46**, 4713–4715.

139 N. Goswami, Q. Yao, T. Chen and J. Xie, Mechanistic exploration and controlled synthesis of precise thiolate-gold nanoclusters, *Coord. Chem. Rev.*, 2016, **329**, 1–15.

140 M. Brust, J. Fink, D. Bethell, D. J. Schiffrin and C. Kiely, Synthesis and reactions of functionalised gold nanoparticles, *J. Chem. Soc., Chem. Commun.*, 1995, **16**, 1655–1656.

141 Z. Wu, J. Chen and R. Jin, One-Pot Synthesis of $Au_{25}(SG)_{18}$ 2- and 4-nm Gold Nanoparticles and Comparison of Their Size-Dependent Properties, *Adv. Funct. Mater.*, 2011, **21**, 177–183.

142 Y. Negishi and T. Tsukuda, One-Pot Preparation of Subnanometer-Sized Gold Clusters via Reduction and Stabilization by meso-2,3-Dimercaptosuccinic Acid, *J. Am. Chem. Soc.*, 2003, **125**, 4046–4047.

143 J. Kim, K. Lema, M. Ukaigwe and D. Lee, Facile Preparative Route to Alkanethiolate-Coated Au_{38} Nanoparticles: Postsynthesis Core Size Evolution, *Langmuir*, 2007, **23**, 7853–7858.

144 Y. Pei, Y. Gao and X. C. Zeng, Structural Prediction of Thiolate-Protected Au_{38}: A Face-Fused Bi-icosahedral Au Core, *J. Am. Chem. Soc.*, 2008, **130**, 7830–7832.

145 H. Qian, W. T. Eckenhoff, Y. Zhu, T. Pintauer and R. Jin, Total Structure Determination of Thiolate-Protected Au_{38} Nanoparticles, *J. Am. Chem. Soc.*, 2010, **132**, 8280–8281.

146 L. Beqa, D. Deschamps, S. Perrio, A.-C. Gaumont, S. Knoppe and T. Bürgi, Ligand Exchange Reaction on $Au_{38}(SR)_{24}$, Separation of $Au_{38}(SR)_{23}(SR')_1$ Regioisomers, and Migration of Thiolates, *J. Phys. Chem. C*, 2013, **117**, 21619–21625.

147 S. Knoppe, S. Michalet and T. Bürgi, Stabilization of Thiolate-Protected Gold Clusters Against Thermal Inversion: Diastereomeric $Au_{38}(SCH_2CH_2Ph)_{24-2x}(R\text{-}BINAS)_x$, *J. Phys. Chem. C*, 2013, **117**, 15354–15361.

148 T. Dainese, S. Antonello, S. Bogialli, W. Fei, A. Venzo and F. Maran, Gold Fusion: From $Au_{25}(SR)_{18}$ to $Au_{38}(SR)_{24}$, the Most Unexpected Transformation of a Very Stable Nanocluster, *ACS Nano*, 2018, **12**, 7057–7066.

149 M. Zhou, J. Zhong, S. Wang, Q. Guo, M. Zhu, Y. Pei and A. Xia, *J. Phys. Chem. C*, 2015, **119**, 18790–18797.

150 A. Dass, S. Theivendran, P. R. Nimmala, C. Kumara, V. R. Jupally, A. Fortunelli, L. Sementa, G. Barcaro, X. Zuo and B. C. Noll, $Au_{133}(SPh\text{-}tBu)_{52}$ Nanomolecules: X-ray Crystallography, Optical, Electrochemical, and Theoretical Analysis, *J. Am. Chem. Soc.*, 2015, **137**, 4610–4613.

151 X. K. Wan, W. W. Xu, S. F. Yuan, Y. Gao, X. C. Zeng and Q. M. Wang, A Near-Infrared-Emissive Alkynyl-Protected

Au_{24} Nanocluster, *Angew. Chem., Int. Ed.*, 2015, **54**, 9683–9686.

152 T. Higaki, C. Liu, M. Zhou, T. Y. Luo, N. L. Rosi and R. Jin, Tailoring the Structure of 58-Electron Gold Nanoclusters: $Au_{103}S_2$(S-Nap)$_{41}$ and Its Implications, *J. Am. Chem. Soc.*, 2017, **139**, 9994–10001.

153 S. Kenzler, C. Schrenk and A. Schnepf, $Au_{108}S_{24}(PPh_3)_{16}$: A Highly Symmetric Nanoscale Gold Cluster Confirms the General Concept of Metalloid Clusters, *Angew. Chem., Int. Ed.*, 2017, **56**, 393–396.

154 N. A. Sakthivel, S. Theivendran, V. Ganeshraj, A. G. Oliver and A. Dass, Crystal Structure of Faradaurate-279: Au_{279}(SPh-tBu)$_{84}$ Plasmonic Nanocrystal Molecules, *J. Am. Chem. Soc.*, 2017, **139**, 15450–15459.

155 N. Yan, N. Xia, L. Liao, M. Zhu, F. Jin, R. Jin and Z. Wu, Unraveling the long-pursued Au_{144} structure by x-ray crystallography, *Sci. Adv.*, 2018, **4**, eaat7259.

156 J.-J. Li, Z.-J. Guan, Z. Lei, F. Hu and Q.-M. Wang, Same Magic Number but Different Arrangement: Alkynyl-Protected Au_{25} with D3 Symmetry, *Angew. Chem., Int. Ed.*, 2019, **58**, 1083–1087.

157 H. Shen, G. Deng, S. Kaappa, T. Tan, Y.-Z. Han, S. Malola, S.-C. Lin, B. K. Teo, H. Häkkinen and N. Zheng, Highly Robust but Surface-Active: N-Heterocyclic Carbene-Stabilized Au_{25} Nanocluster, *Angew. Chem., Int. Ed.*, 2019, **58**, 17731–17735.

158 S. Bestgen, O. Fuhr, B. Breitung, V. S. Kiran Chakravadhanula, G. Guthausen, F. Hennrich, W. Yu, M. M. Kappes, P. W. Roesky and D. Fenske, $[Ag_{115}S_{34}(SCH_2C_6H_4tBu)_{47}(dpph)_6]$: synthesis, crystal structure and NMR investigations of a soluble silver chalcogenide nanocluster, *Chem. Sci.*, 2017, **8**, 2235–2240.

159 Z.-Y. Chen, D. Y. S. Tam and T. C. W. Mak, Chloride assisted supramolecular assembly of a luminescent gigantic cluster: $[Ag_{216}S_56Cl_7(C{\equiv}CPh)_{98}(H_2O)_{12}]^-$ with pseudo-Th skeleton and five-shell arrangement, *Nanoscale*, 2017, **9**, 8930–8937.

160 P. Chakraborty, A. Nag, G. Paramasivam, G. Natarajan and T. Pradeep, Fullerene-Functionalized Monolayer-Protected Silver Clusters: $[Ag_{29}(BDT)_{12}(C_{60})_n]^{3-}$ (n = 1-9), *ACS Nano*, 2018, **12**, 2415–2425.

161 J. W. Liu, L. Feng, H. F. Su, Z. Wang, Q. Q. Zhao, X. P. Wang, C. H. Tung, D. Sun and L. S. Zheng, Anisotropic Assembly of Ag_{52} and Ag_{76} Nanoclusters, *J. Am. Chem. Soc.*, 2018, **140**, 1600–1603.

162 Y. Song, K. Lambright, M. Zhou, K. Kirschbaum, J. Xiang, A. Xia, M. Zhu and R. Jin, Large-Scale Synthesis, Crystal Structure, and Optical Properties of the $Ag_{146}Br_2(SR)_{80}$ Nanocluster, *ACS Nano*, 2018, **12**, 9318–9325.

163 Z. Wang, H. F. Su, M. Kurmoo, C. H. Tung, D. Sun and L. S. Zheng, Trapping an octahedral Ag_6 kernel in a seven-fold symmetric Ag_{56} nanowheel, *Nat. Commun.*, 2018, **9**, 2094.

164 J. W. Liu, Z. Wang, Y. M. Chai, M. Kurmoo, Q. Q. Zhao, X. P. Wang, C. H. Tung and D. Sun, Core Modulation of 70-Nuclei Core-Shell Silver Nanoclusters, *Angew. Chem., Int. Ed.*, 2019, **58**, 6276–6279.

165 W. Du, S. Deng, S. Chen, S. Jin, Y. Zhen, Y. Pei and M. Zhu, Anisotropic Evolution of Nanoclusters from Ag_{40} to Ag_{45}: Halogen- and Defect-Induced Epitaxial Growth in Nanoclusters, *J. Phys. Chem. Lett.*, 2021, **12**, 6654–6660.

166 L. V. Nair, S. Hossain, S. Wakayama, S. Takagi, M. Yoshioka, J. Maekawa, A. Harasawa, B. Kumar, Y. Niihori, W. Kurashige and Y. Negishi, $[Pt_{17}(CO)_{12}(PPh_3)_8]^{n+}$ (n = 1, 2): Synthesis and Geometric and Electronic Structures, *J. Phys. Chem. C*, 2017, **121**, 11002–11009.

167 A. Ghosh, R.-W. Huang, B. Alamer, E. Abou-Hamad, M. N. Hedhili, O. F. Mohammed and O. M. Bakr, $[Cu_{61}(StBu)_{26}S_6Cl_6H_{14}]^+$: A Core-Shell Superatom Nanocluster with a Quasi-J_{36} Cu_{19} Core and an "18-Crown-6" Metal-Sulfide-like Stabilizing Belt, *ACS Mater. Lett.*, 2019, **1**, 297–302.

168 A. Baghdasaryan, C. Besnard, L. M. Lawson Daku, T. Delgado and T. Burgi, Thiolato Protected Copper Sulfide Cluster with the Tentative Composition $Cu_{74}S_{15}$(2-PET)$_{45}$, *Inorg. Chem.*, 2020, **59**, 2200–2208.

169 R.-W. Huang, J. Yin, C. Dong, A. Ghosh, M. J. Alhilaly, X. Dong, M. N. Hedhili, E. Abou-Hamad, B. Alamer, S. Nematulloev, Y. Han, O. F. Mohammed and O. M. Bakr, $[Cu_{81}(PhS)_{46}(tBuNH_2)_{10}(H)_{32}]^{3+}$ Reveals the Coexistence of Large Planar Cores and Hemispherical Shells in High-Nuclearity Copper Nanoclusters, *J. Am. Chem. Soc.*, 2020, **142**, 8696–8705.

170 S. Nematulloev, R. W. Huang, J. Yin, A. Shkurenko, C. Dong, A. Ghosh, B. Alamer, R. Naphade, M. N. Hedhili, P. Maity, M. Eddaoudi, O. F. Mohammed and O. M. Bakr, $[Cu_{15}(PPh_3)_6(PET)_{13}]^{2+}$: a Copper Nanocluster with Crystallization Enhanced Photoluminescence, *Small*, 2021, **17**, e2006839.

171 G. H. Woehrle and J. E. Hutchison, Thiol-Functionalized Undecagold Clusters by Ligand Exchange: Synthesis, Mechanism, and Properties, *Inorg. Chem.*, 2005, **44**, 6149–6158.

172 W. Kurashige, M. Yamaguchi, K. Nobusada and Y. Negishi, Ligand-Induced Stability of Gold Nanoclusters: Thiolate versus Selenolate, *J. Phys. Chem. Lett.*, 2012, **3**, 2649–2652.

173 M. S. Bootharaju, C. P. Joshi, M. J. Alhilaly and O. M. Bakr, Switching a Nanocluster Core from Hollow to Nonhollow, *Chem. Mater.*, 2016, **28**, 3292–3297.

174 X. Zou, S. Jin, W. Du, Y. Li, P. Li, S. Wang and M. Zhu, Multi-ligand-directed synthesis of chiral silver nanoclusters, *Nanoscale*, 2017, **9**, 16800–16805.

175 X. Kang and M. Zhu, Transformation of Atomically Precise Nanoclusters by Ligand-Exchange, *Chem. Mater.*, 2019, **31**, 9939–9969.

176 L. He and T. Dong, Progress in controlling the synthesis of atomically precise silver nanoclusters, *CrystEngComm*, 2021, **23**, 7369–7379.

177 D. E. Bergeron, O. Coskuner, J. W. Hudgens and C. A. Gonzalez, Ligand Exchange Reactions in the Formation of Diphosphine-Protected Gold Clusters, *J. Phys. Chem. C*, 2008, **112**, 12808–12814.

178 M. R. Narouz, K. M. Osten, P. J. Unsworth, R. W. Y. Man, K. Salorinne, S. Takano, R. Tomihara, S. Kaappa, S. Malola,

C.-T. Dinh, J. D. Padmos, K. Ayoo, P. J. Garrett, M. Nambo, J. H. Horton, E. H. Sargent, H. Häkkinen, T. Tsukuda and C. M. Crudden, N-heterocyclic carbene-functionalized magic-number gold nanoclusters, *Nat. Chem.*, 2019, **11**, 419–425.

179 S. Si, C. Gautier, J. Boudon, R. Taras, S. Gladiali and T. Bürgi, Ligand Exchange on Au_{25} Cluster with Chiral Thiols, *J. Phys. Chem. C*, 2009, **113**, 12966–12969.

180 C. Zeng, C. Liu, Y. Pei and R. Jin, Thiol Ligand-Induced Transformation of $Au_{38}(SC_2H_4Ph)_{24}$ to Au_{36}(SPh-t-Bu)$_{24}$, *ACS Nano*, 2013, **7**, 6138–6145.

181 T. M. Carducci, R. E. Blackwell and R. W. Murray, Charge-Transfer Effects in Ligand Exchange Reactions of Au_{25} Monolayer-Protected Clusters, *J. Phys. Chem. Lett.*, 2015, **6**, 1299–1302.

182 A. Fernando and C. M. Aikens, Deciphering the Ligand Exchange Process on Thiolate Monolayer Protected $Au_{38}(SR)_{24}$ Nanoclusters, *J. Phys. Chem. C*, 2016, **120**, 14948–14961.

183 S. K. Eswaramoorthy, N. A. Sakthivel and A. Dass, Core Size Conversion of $Au_{329}(SCH_2CH_2Ph)_{84}$ to Au_{279}(SPh-tBu)$_{84}$ Nanomolecules, *J. Phys. Chem. C*, 2019, **123**, 9634–9639.

184 A. George, A. Sundar, A. S. Nair, M. P. Maman, B. Pathak, N. Ramanan and S. Mandal, Identification of Intermediate $Au_{22}(SR)_4(SR')_{14}$ Cluster on Ligand-Induced Transformation of $Au_{25}(SR)_{18}$ Nanocluster, *J. Phys. Chem. Lett.*, 2019, **10**, 4571–4576.

185 M.-B. Li, S.-K. Tian, Z. Wu and R. Jin, Peeling the Core-Shell Au_{25} Nanocluster by Reverse Ligand-Exchange, *Chem. Mater.*, 2016, **28**, 1022–1025.

186 C. A. Hosier and C. J. Ackerson, Regiochemistry of Thiolate for Selenolate Ligand Exchange on Gold Clusters, *J. Am. Chem. Soc.*, 2019, **141**, 309–314.

187 L. O. Brown and J. E. Hutchison, Convenient Preparation of Stable, Narrow-Dispersity, Gold Nanocrystals by Ligand Exchange Reactions, *J. Am. Chem. Soc.*, 1997, **119**, 12384–12385.

188 C. Zeng, H. Qian, T. Li, G. Li, N. L. Rosi, B. Yoon, R. N. Barnett, R. L. Whetten, U. Landman and R. Jin, Total structure and electronic properties of the gold nanocrystal $Au_{36}(SR)_{24}$, *Angew. Chem., Int. Ed.*, 2012, **51**, 13114–13118.

189 N. Xia, J. Yuan, L. Liao, W. Zhang, J. Li, H. Deng, J. Yang and Z. Wu, Structural Oscillation Revealed in Gold Nanoparticles, *J. Am. Chem. Soc.*, 2020, **142**, 12140–12145.

190 W. T. Chang, P. Y. Lee, J. H. Liao, K. K. Chakrahari, S. Kahlal, Y. C. Liu, M. H. Chiang, J. Y. Saillard and C. W. Liu, Eight-Electron Silver and Mixed Gold/Silver Nanoclusters Stabilized by Selenium Donor Ligands, *Angew. Chem., Int. Ed.*, 2017, **56**, 10178–10182.

191 P. R. Nimmala and A. Dass, $Au_{99}(SPh)_{42}$ nanomolecules: aromatic thiolate ligand induced conversion of $Au_{144}(SCH_2CH_2Ph)_{60}$, *J. Am. Chem. Soc.*, 2014, **136**, 17016–17023.

192 P. R. Nimmala, S. Theivendran, G. Barcaro, L. Sementa, C. Kumara, V. R. Jupally, E. Apra, M. Stener, A. Fortunelli and A. Dass, Transformation of $Au_{144}(SCH_2CH_2Ph)_{60}$ to $Au_{133}(SPh\text{-}tBu)_{52}$ Nanomolecules: Theoretical and Experimental Study, *J. Phys. Chem. Lett.*, 2015, **6**, 2134–2139.

193 C. Zeng, C. Liu, Y. Chen, N. L. Rosi and R. Jin, Gold-thiolate ring as a protecting motif in the $Au_{20}(SR)_{16}$ nanocluster and implications, *J. Am. Chem. Soc.*, 2014, **136**, 11922–11925.

194 C. Zeng, T. Li, A. Das, N. L. Rosi and R. Jin, Chiral structure of thiolate-protected 28-gold-atom nanocluster determined by X-ray crystallography, *J. Am. Chem. Soc.*, 2013, **135**, 10011–10013.

195 Z. Gan, Y. Lin, L. Luo, G. Han, W. Liu, Z. Liu, C. Yao, L. Weng, L. Liao, J. Chen, X. Liu, Y. Luo, C. Wang, S. Wei and Z. Wu, Fluorescent Gold Nanoclusters with Interlocked Staples and a Fully Thiolate-Bound Kernel, *Angew. Chem., Int. Ed.*, 2016, **55**, 11567–11571.

196 A. Das, T. Li, G. Li, K. Nobusada, C. Zeng, N. L. Rosi and R. Jin, Crystal structure and electronic properties of a thiolate-protected Au_{24} nanocluster, *Nanoscale*, 2014, **6**, 6458–6462.

197 M. Rambukwella, L. Sementa, A. Fortunelli and A. Dass, Core-Size Conversion of $Au_{38}(SCH_2CH_2Ph)_{24}$ to Au30(S–tBu)18 Nanomolecules, *J. Phys. Chem. C*, 2017, **121**, 14929–14935.

198 Z. Gan, J. Chen, L. Liao, H. Zhang and Z. Wu, Surface Single Atom Tailoring of Gold Nanoparticle, *J. Phys. Chem. Lett.*, 2018, **9**, 204–208.

199 A. Dass, T. C. Jones, S. Theivendran, L. Sementa and A. Fortunelli, Core Size Interconversions of $Au_{30}(S\text{-}tBu)_{18}$ and $Au_{36}(SPhX)_{24}$, *J. Phys. Chem. C*, 2017, **121**, 14914–14919.

200 A. Ghosh, D. Ghosh, E. Khatun, P. Chakraborty and T. Pradeep, Unusual reactivity of dithiol protected clusters in comparison to monothiol protected clusters: studies using $Ag_{51}(BDT)_{19}(TPP)_3$ and $Ag_{29}(BDT)_{12}(TPP)_4$, *Nanoscale*, 2017, **9**, 1068–1077.

201 E. Khatun, A. Ghosh, D. Ghosh, P. Chakraborty, A. Nag, B. Mondal, S. Chennu and T. Pradeep, $[Ag_{59}(2,5\text{-}DCBT)_{32}]^{3-}$: a new cluster and a precursor for three well-known clusters, *Nanoscale*, 2017, **9**, 8240–8248.

202 M. S. Bootharaju, V. M. Burlakov, T. M. D. Besong, C. P. Joshi, L. G. AbdulHalim, D. M. Black, R. L. Whetten, A. Goriely and O. M. Bakr, Reversible Size Control of Silver Nanoclusters via Ligand-Exchange, *Chem. Mater.*, 2015, **27**, 4289–4297.

203 H. Qian, Y. Zhu and R. Jin, Size-Focusing Synthesis, Optical and Electrochemical Properties of Monodisperse $Au_{38}(SC_2H_4Ph)_{24}$ Nanoclusters, *ACS Nano*, 2009, **3**, 3795–3803.

204 S. Jin, S. Wang, Y. Song, M. Zhou, J. Zhong, J. Zhang, A. Xia, Y. Pei, M. Chen, P. Li and M. Zhu, Crystal structure and optical properties of the $[Ag_{62}S_{12}(SBu(t))_{32}]^{2+}$ nanocluster with a complete face-centered cubic kernel, *J. Am. Chem. Soc.*, 2014, **136**, 15559–15565.

205 E. S. Shibu, M. A. H. Muhammed, T. Tsukuda and T. Pradeep, Ligand Exchange of $Au_{25}SG_{18}$ Leading to Functionalized Gold Clusters: Spectroscopy, Kinetics, and Luminescence, *J. Phys. Chem. C*, 2008, **112**, 12168–12176.

206 Y. Zhao, S. Zhuang, L. Liao, C. Wang, N. Xia, Z. Gan, W. Gu, J. Li, H. Deng and Z. Wu, A Dual Purpose Strategy to Endow

Gold Nanoclusters with Both Catalysis Activity and Water Solubility, *J. Am. Chem. Soc.*, 2020, **142**, 973–977.

207 S. Yang, J. Chai, Y. Song, J. Fan, T. Chen, S. Wang, H. Yu, X. Li and M. Zhu, In Situ Two-Phase Ligand Exchange: A New Method for the Synthesis of Alloy Nanoclusters with Precise Atomic Structures, *J. Am. Chem. Soc.*, 2017, **139**, 5668–5671.

208 J. Chai, S. Yang, Y. Lv, H. Chong, H. Yu and M. Zhu, Exposing the Delocalized Cu-S π Bonds on the Au_{24}-$Cu_6(SPhtBu)_{22}$ Nanocluster and Its Application in Ring-Opening Reactions, *Angew. Chem., Int. Ed.*, 2019, **58**, 15671–15674.

209 X. Liu and D. Astruc, From Galvanic to Anti-Galvanic Synthesis of Bimetallic Nanoparticles and Applications in Catalysis, Sensing, and Materials Science, *Adv. Mater.*, 2017, **29**, 1605305.

210 Z. Gan, N. Xia and Z. Wu, Discovery, Mechanism, and Application of Antigalvanic Reaction, *Acc. Chem. Res.*, 2018, **51**, 2774–2783.

211 C. M. Cobley and Y. Xia, Engineering the properties of metal nanostructures via galvanic replacement reactions, *Mater. Sci. Eng., R*, 2010, **70**, 44–62.

212 A. G. M. da Silva, T. S. Rodrigues, S. J. Haigh and P. H. C. Camargo, Galvanic replacement reaction: recent developments for engineering metal nanostructures towards catalytic applications, *Chem. Commun.*, 2017, **53**, 7135–7148.

213 T. Udayabhaskararao, Y. Sun, N. Goswami, S. K. Pal, K. Balasubramanian and T. Pradeep, Ag_7Au_6: A 13-Atom Alloy Quantum Cluster, *Angew. Chem., Int. Ed.*, 2012, **51**, 2155–2159.

214 Q. Yao, Y. Feng, V. Fung, Y. Yu, D. E. Jiang, J. Yang and J. Xie, Precise control of alloying sites of bimetallic nanoclusters via surface motif exchange reaction, *Nat. Commun.*, 2017, **8**, 1555.

215 L. He, Z. Gan, N. Xia, L. Liao and Z. Wu, Alternating Array Stacking of $Ag_{26}Au$ and $Ag_{24}Au$ Nanoclusters, *Angew. Chem., Int. Ed.*, 2019, **58**, 9897–9901.

216 X. Kang, S. Chen, S. Jin, Y. Song, Y. Xu, H. Yu, H. Sheng and M. Zhu, Heteroatom Effects on the Optical and Electrochemical Properties of $Ag_{25}(SR)_{18}$ and Its Dopants, *ChemElectroChem*, 2016, **3**, 1261–1265.

217 M. S. Bootharaju, L. Sinatra and O. M. Bakr, Distinct metal-exchange pathways of doped Ag_{25} nanoclusters, *Nanoscale*, 2016, **8**, 17333–17339.

218 X. Kang, L. Xiong, S. Wang, H. Yu, S. Jin, Y. Song, T. Chen, L. Zheng, C. Pan, Y. Pei and M. Zhu, Shape-Controlled Synthesis of Trimetallic Nanoclusters: Structure Elucidation and Properties Investigation, *Chem. – Eur. J.*, 2016, **22**, 17145–17150.

219 M. Zhu, P. Wang, N. Yan, X. Chai, L. He, Y. Zhao, N. Xia, C. Yao, J. Li, H. Deng, Y. Zhu, Y. Pei and Z. Wu, The Fourth Alloying Mode by Way of Anti-Galvanic Reaction, *Angew. Chem., Int. Ed.*, 2018, **57**, 4500–4504.

220 J.-P. Choi, C. A. Fields-Zinna, R. L. Stiles, R. Balasubramanian, A. D. Douglas, M. C. Crowe and R. W. Murray, Reactivity of $[Au_{25}(SCH_2CH_2Ph)_{18}]^{1-}$ Nanoparticles with Metal Ions, *J. Phys. Chem. C*, 2010, **114**, 15890–15896.

221 Z. K. Wu, Anti-Galvanic Reduction of Thiolate-Protected Gold and Silver Nanoparticles, *Angew. Chem., Int. Ed.*, 2012, **51**, 2934–2938.

222 M. Wang, Z. Wu, Z. Chu, J. Yang and C. Yao, Chemico-Physical Synthesis of Surfactant- and Ligand-Free Gold Nanoparticles and Their Anti-Galvanic Reduction Property, *Chem. – Asian J.*, 2014, **9**, 1006–1010.

223 W. Zhang, S. Zhuang, L. Liao, H. Dong, N. Xia, J. Li, H. Deng and Z. Wu, Two-Way Alloying and Dealloying of Cadmium in Metalloid Gold Clusters, *Inorg. Chem.*, 2019, **58**, 5388–5392.

224 S. Wang, Y. Song, S. Jin, X. Liu, J. Zhang, Y. Pei, X. Meng, M. Chen, P. Li and M. Zhu, Metal exchange method using Au_{25} nanoclusters as templates for alloy nanoclusters with atomic precision, *J. Am. Chem. Soc.*, 2015, **137**, 4018–4021.

225 S. Yang, S. Wang, S. Jin, S. Chen, H. Sheng and M. Zhu, A metal exchange method for thiolate-protected tri-metal M_1-$Ag_xAu_{24-x}(SR)_{18}^0$ (M = Cd/Hg) nanoclusters, *Nanoscale*, 2015, **7**, 10005–10007.

226 S. Hossain, T. Ono, M. Yoshioka, G. Hu, M. Hosoi, Z. Chen, L. V. Nair, Y. Niihori, W. Kurashige, D.-e. Jiang and Y. Negishi, Thiolate-Protected Trimetallic Au approximately 20Ag approximately 4Pd and Au approximately 20Ag approximately 4Pt Alloy Clusters with Controlled Chemical Composition and Metal Positions, *J. Phys. Chem. Lett.*, 2018, **9**, 2590–2594.

227 S. Wang, H. Abroshan, C. Liu, T. Y. Luo, M. Zhu, H. J. Kim, N. L. Rosi and R. Jin, Shuttling single metal atom into and out of a metal nanoparticle, *Nat. Commun.*, 2017, **8**, 848.

228 C. Yao, C.-Q. Xu, I.-H. Park, M. Zhao, Z. Zhu, J. Li, X. Hai, H. Fang, Y. Zhang, G. Macam, J. Teng, L. Li, Q.-H. Xu, F.-C. Chuang, J. Lu, C. Su, J. Li and J. Lu, Giant Emission Enhancement of Solid-State Gold Nanoclusters by Surface Engineering, *Angew. Chem., Int. Ed.*, 2020, **59**, 8270–8276.

229 J. P. Wilcoxon and B. L. Abrams, Synthesis, structure and properties of metal nanoclusters, *Chem. Soc. Rev.*, 2006, **35**, 1162–1194.

230 H. W. Duan and S. M. Nie, Etching Colloidal Gold Nanocrystals with Hyperbranched and Multivalent Polymers: A New Route to Fluorescent and Water-Soluble Atomic Clusters, *J. Am. Chem. Soc.*, 2007, **129**, 2412–2413.

231 N. Xia, Z. Gan, L. Liao, S. Zhuang and Z. Wu, The reactivity of phenylethanethiolated gold nanoparticles with acetic acid, *Chem. Commun.*, 2017, **53**, 11646–11649.

232 H. Qian and R. Jin, Controlling Nanoparticles with Atomic Precision: The Case of $Au_{144}(SCH_2CH_2Ph)_{60}$, *Nano Lett.*, 2009, **9**, 4083–4087.

233 T. U. B. Rao, B. Nataraju and T. Pradeep, Ag_9 Quantum Cluster through a Solid-State Route, *J. Am. Chem. Soc.*, 2010, **132**, 16304–16307.

234 I. Chakraborty, A. Govindarajan, J. Erusappan, A. Ghosh, T. Pradeep, B. Yoon, R. L. Whetten and U. Landman, The Superstable 25 kDa Monolayer Protected Silver Nanoparticle: Measurements and Interpretation as an Icosahedral $Ag_{152}(SCH_2CH_2Ph)_{60}$ Cluster, *Nano Lett.*, 2012, **12**, 5861–5866.

235 I. Chakraborty, T. Udayabhaskararao, G. K. Deepesh and T. Pradeep, Sunlight mediated synthesis and antibacterial properties of monolayer protected silver clusters, *J. Mater. Chem. B*, 2013, **1**, 4059–4064.

236 I. Chakraborty, S. Mahata, A. Mitra, G. De and T. Pradeep, Controlled synthesis and characterization of the elusive thiolated Ag_{55} cluster, *Dalton Trans.*, 2014, **43**, 17904–17907.

237 O. M. Bakr, V. Amendola, C. M. Aikens, W. Wenseleers, R. Li, L. Dal Negro, G. C. Schatz and F. Stellacci, Silver nanoparticles with broad multiband linear optical absorption, *Angew. Chem., Int. Ed.*, 2009, **48**, 5921–5926.

238 A. Desireddy, B. E. Conn, J. Guo, B. Yoon, R. N. Barnett, B. M. Monahan, K. Kirschbaum, W. P. Griffith, R. L. Whetten, U. Landman and T. P. Bigioni, Ultrastable silver nanoparticles, *Nature*, 2013, **501**, 399–402.

239 K. R. Krishnadas, A. Ghosh, A. Baksi, I. Chakraborty, G. Natarajan and T. Pradeep, Intercluster Reactions between $Au_{25}(SR)_{18}$ and $Ag_{44}(SR)_{30}$, *J. Am. Chem. Soc.*, 2016, **138**, 140–148.

240 S. Bhat, A. Baksi, S. K. Mudedla, G. Natarajan, V. Subramanian and T. Pradeep, $Au_{22}Ir_3(PET)_{18}$: An Unusual Alloy Cluster through Intercluster Reaction, *J. Phys. Chem. Lett.*, 2017, **8**, 2787–2793.

241 E. Khatun, P. Chakraborty, B. R. Jacob, G. Paramasivam, M. Bodiuzzaman, W. A. Dar and T. Pradeep, Intercluster Reactions Resulting in Silver-Rich Trimetallic Nanoclusters, *Chem. Mater.*, 2020, **32**, 611–619.

242 N. Xia and Z. Wu, Doping Au_{25} nanoparticles using ultrasmall silver or copper nanoparticles as the metal source, *J. Mater. Chem. C*, 2016, **4**, 4125–4128.

